Kelemen, P.B., Kikawa, E., and Miller, D.J. (Eds.)
Proceedings of the Ocean Drilling Program, Scientific Results Volume 209

1. Leg 209 Summary: Processes in a 20-km-Thick Conductive Boundary Layer beneath the Mid-Atlantic Ridge, 14°–16°N[1]

Peter B. Kelemen,[2] Eiichi Kikawa,[3] D. Jay Miller,[4] and Shipboard Scientific Party[5]

ABSTRACT

This paper provides a summary of postcruise scientific results from Ocean Drilling Program (ODP) Leg 209 available to date, building upon shipboard observations and syntheses summarized in the Leg 209 *Initial Results* volume. During Leg 209, 19 holes were drilled at 8 sites along the Mid-Atlantic Ridge from 14°43′ to 15°44′N, mainly in residual mantle peridotite intruded by gabbroic rocks, in order to understand the tectonic and structural processes responsible for formation of oceanic lithosphere with abundant residual peridotite exposed on the seafloor coupled with a relatively low proportion of volcanic rocks.

Based on proportions of recovered lithologies, the entire area may be underlain by mantle peridotite with ~20%–40% gabbroic intrusions and impregnations. Impregnated peridotites with olivine + two pyroxenes + plagioclase + spinel that apparently formed in equilibrium probably record crystallization from primitive mid-ocean-ridge basalt at pressures of 0.5–0.6 GPa. Metamorphic equilibria record isobaric cooling to ~1100°C at this pressure. Thus, the conductively cooled thermal boundary layer beneath the Mid-Atlantic Ridge in this region is >15 km thick.

Combined crystallization and reaction with residual peridotite formed a series of impregnated peridotites recording increasing Na content at nearly constant Mg#; this process could explain some of the variation in fractionation-corrected Na (e.g., Na = 8.0) observed in mid-

[1]Kelemen, P.B., Kikawa, E., Miller, D.J., and Shipboard Scientific Party, 2007. Leg 209 summary: processes in a 20-km-thick conductive boundary layer beneath the Mid-Atlantic Ridge, 14°–16°N. *In* Kelemen, P.B., Kikawa, E., and Miller, D.J. (Eds.), *Proc. ODP, Sci. Results,* 209: College Station, TX (Ocean Drilling Program), 1–33. doi:10.2973/odp.proc.sr.209.001.2007
[2]Department of Earth and Environmental Sciences, Lamont-Doherty Earth Observatory of Columbia University, PO Box 1000, 61 Route 9W, Palisades NY 10964, USA. **peterk@ldeo.columbia.edu**
[3]Deep Sea Research Department, Japan Agency for Marine-Earth Science and Technology, 2-15 Natsushima-cho, Yokosuka 237-0061, Japan.
[4]Integrated Ocean Drilling Program, Texas A&M University, 1000 Discovery Drive, College Station TX 77845-9547, USA.
[5]**Shipboard Scientific Party addresses.**

Initial receipt: 19 January 2007
Acceptance: 10 April 2007
Web publication: 7 June 2007
Ms 209SR-001

ocean-ridge basalts. Clinopyroxene textures and compositions record such impregnation processes, and they are particularly well documented for Site 1274. Other Leg 209 gabbroic rocks formed from extensive crystallization of highly evolved melts, indicating that a substantial proportion of melt entering the thermal boundary layer crystallizes entirely beneath the seafloor, with no volcanic equivalent.

Alteration of peridotites occurred over a range of temperatures and is the result of three distinct processes: rock-dominated serpentinization with formation of brucite in olivine-rich lithologies, fluid-dominated serpentinization with formation of magnetite and no brucite, and fluid-dominated talc alteration with addition of SiO_2 as well as H_2O and oxygen. The latter two processes also exhibit detectable trace element metasomatism that is distinct in its character from the igneous impregnation described in the previous paragraph.

Microstructures show that most residual peridotites were not ductilely deformed at temperatures less than ~1200°C. Structural and paleomagnetic data require tectonic rotations of relatively undeformed blocks; some rotations probably exceeded 60° around nearly horizontal axes parallel to the rift axis. Rotations occurred along several generations of high-temperature mylonitic shear zones extending deeper than 15 km depth and numerous faults at lower temperature. Early formed shear zones and faults were passively rotated around later features; such a process could have produced low-angle fault surfaces without slip on low-angle faults. This region provides end-member examples of processes that are common at many or most slow-spreading ridges.

Osmium isotope ratios indicate an ancient history of depletion for residual peridotites from the 14°–16°N region along the Mid-Atlantic Ridge. Though depleted Os isotope ratios in peridotite have been reported elsewhere along the global ridge system, the values from this region are among the most depleted. In general, Os isotope ratios from mid-ocean-ridge basalts are systematically more radiogenic than Os isotope ratios from ridge peridotite samples, suggesting a polygenetic heterogeneous source for mid-ocean-ridge basalts.

Geochemical studies of zircons from Leg 209 gabbroic rocks and impregnated peridotites, together with other ridge and arc-related zircons, indicate that ridge zircons have systematically lower fractionation-corrected U and Th concentrations compared to arc zircons. This observation provides a tool for interpreting the tectonic provenance of ancient detrital zircons and indicates an arclike provenance for Hadean detrital zircons.

Geobiological studies and aerobiological studies were also undertaken during Leg 209. The geobiological work found no measurable microbial enhancement of olivine dissolution rate, possibly because the samples from Leg 209 were sterile. The aerobiological study determined that dust from North Africa, collected from the derrick of the *JOIDES Resolution* during Leg 209, contains a variety of abundant microorganisms.

INTRODUCTION

This short paper provides a summary of postcruise scientific results from Ocean Drilling Program (ODP) Leg 209 available to date, building upon shipboard observations and synthesis summarized in Kelemen, Kikawa, Miller, et al. (2004). Emphasis is placed upon published and submitted papers, although in a few cases these are supplemented by data and interpretations published only in abstract form. The paper is organized by discipline, beginning with those most central to the primary goals of the leg. Discussion and conclusions are offered within each disciplinary group rather than in a comprehensive section at the end of the paper.

In addition to this summary, a Leg 209 scientific synthesis paper was submitted to both *Science*, where it was not reviewed, and to *Nature*. Efforts continue to publish this paper, which is currently in revision as a *Letter to Nature* (Kelemen et al., submitted [**N1**]). Meanwhile, the reader is directed to the syntheses available in Kelemen, Kikawa, Miller, et al. (2004) for a more thorough treatment of the overall results of Leg 209.

Understanding the creation of oceanic plates at spreading ridges provides the simplest template for understanding creation and evolution of Earth's crust and shallow mantle in all tectonic settings. Some aspects of ridge processes are clear; for example, it is established that plate spreading drives mantle upwelling and leads to decompression melting, which in turn forms igneous crust. However, fundamental differences exist between oceanic plates formed at "fast-spreading" ridges (>2 cm/yr half-rate) versus those formed at "slow-spreading" ridges (<2 cm/yr half-rate) that are not well understood. Seafloor topography, fractionation-corrected lava compositions, seismic crustal thickness, and topographically corrected gravity anomalies are all more variable at slow-spreading ridges compared to fast-spreading ridges, but the reasons for these differences remain unclear. Unresolved debate over the past two decades has focused on the pattern of mantle upwelling (two-dimensional, plate-driven corner flow versus melt-buoyancy driven radial diapirs), the causes of fractionation-corrected variation in lava compositions (variation in mantle source temperature versus variation in the depth of crystal fractionation), and the reasons for variable crustal thickness along strike (a short review of these topics is provided in Kelemen, Kikawa, Miller, et al., 2004). ODP Leg 209 was proposed to address these problems, providing constraints via drilling of mantle peridotite intruded by gabbroic plutons and exposed on both sides of the slow-spreading Mid-Atlantic Ridge between 14°43′ and 15°44′N.

During Leg 209, 19 holes were drilled at 8 sites (Fig. **F1**). Sites were previously surveyed by submersible and were <200 m from peridotite or dunite exposed on the seafloor; outcrops of gabbroic rock were also near some sites. Primary goals of Leg 209 were to constrain deformation associated with mantle upwelling and corner flow and mechanisms of melt migration and igneous petrogenesis.

F1. Drill site locations and bathymetry, p. 25.

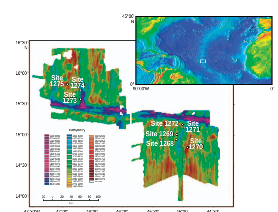

In six holes at Sites 1269 and 1273, we penetrated a total of 112 m of basaltic rubble; recovery was poor (3.7 m total; recovery = 3.3%) and these holes were unstable, so drilling was terminated. Lavas at these sites probably form nearly horizontal surfaces overlying cliffs exposing peridotite and gabbro. These sites will not be discussed further here.

In 13 holes at 6 other sites, we drilled a mixture of residual peridotite and gabbroic rocks intrusive into peridotite. We penetrated a total of 1075 m at these six sites and recovered 354 m of core (recovery = ~33%). This paper reports on postcruise scientific results from these six sites.

Simplified core logs (Fig. **F2**) show that drilling at Sites 1268, 1270, 1271, and 1272 recovered ~25% gabbroic rocks and ~75% residual mantle peridotite (detailed lithologic sections are available in Shipboard Scientific Party, 2004a: figs. F7, F21, F31, F37). Core from Site 1274 is mainly residual peridotite with a few meter-scale gabbroic intrusions (Shipboard Scientific Party, 2004a: fig. F42 and associated text). Core from Site 1275 is mainly gabbroic but contains 24% poikilitic peridotite

F2. Simplified core logs for Leg 209 sites, p. 26.

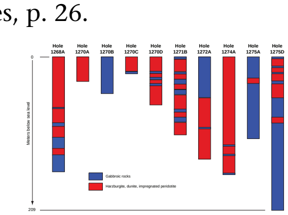

(also known as "troctolite") interpreted as residual peridotite that was "impregnated" by plagioclase and pyroxene crystallized from melt migrating along olivine grain boundaries. These impregnated peridotites were later intruded by evolved gabbros (Shipboard Scientific Party, 2004a: fig. F50 and associated text). Impregnated peridotites form the majority of core from Site 1271 and are present at Sites 1268 and 1270. Thus, we infer that the entire area may be underlain by mantle peridotite with ~20%–40% gabbroic intrusions and impregnations. The overall proportion of gabbroic rocks versus residual peridotites from these six sites is similar to previous dredging and submersible sampling in the area (compiled data and references in Kelemen, Kikawa, Miller, et al., 2004).

IGNEOUS PROCESSES

Thermobarometry

Our synthesis paper (Kelemen et al., submitted [N1]) concentrates on three observations:

1. Compositions of plutonic rocks and primitive mid-ocean-ridge basalt (MORB) samples from the 14°–16°N region along the Mid-Atlantic Ridge are indicative of relatively high pressure crystal fractionation in a 15- to 20-km-thick thermal boundary layer.
2. Most gabbroic rocks sampled during Leg 209 are too evolved to be complementary to crystal fractionation of MORB and may not have a volcanic equivalent. Instead, they may represent crystallization products of melts that solidified entirely in the subsurface, with no volcanic expression.
3. There is a marked lack of crystal shape fabric or other evidence of penetrative subsolidus deformation of residual mantle peridotites recovered during Leg 209, along with a high proportion of ductile shear zones and faults at each site, indicative of localized deformation during seafloor spreading and tectonic denudation of mantle rocks within this 15- to 20-km-thick thermal boundary layer.

In this section, we concentrate on the evidence for igneous crystallization at relatively high pressure.

As reported in the Leg 209 *Initial Results* volume (Kelemen, Kikawa, Miller, et al., 2004), unusual poikilitic peridotites from Site 1275 had "equilibrated" textures prior to low-temperature alteration (Fig. F3). Additional illustrations are available in Shipboard Scientific Party (2004a: fig. F51; 2004g: figs. F6, F18, F40). The poikilitic peridotites contain olivine, orthopyroxene, clinopyroxene, plagioclase, and Cr-rich spinel. Their whole-rock molar Mg/(Mg+Fe), or Mg#, and Ni are high, as are Mg# and Ni contents of olivine and molar Cr/(Cr+Al), or Cr#, of spinel, extending to residual peridotite values. However, plagioclase ranges from 54 to 75 mol% anorthite (Fig. F4), much lower than expected in residual peridotites, particularly because Leg 209 residual peridotites are among the most depleted recovered from the mid-ocean ridges (e.g., Shipboard Scientific Party, 2004f: fig. F51 and accompanying text). The wide range of plagioclase anorthite content in the poikilitic peridotites from Site 1275, at nearly constant olivine Mg# and Ni content, is best understood as the result of "reactive fractionation" involving crystalli-

F3. Poikilitic impregnated peridotite, p. 27.

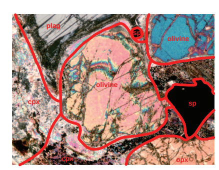

F4. Normative anorthite in plagioclase vs. forsterite in olivines, p. 28.

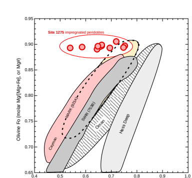

zation during reaction between refractory peridotite and cooling, fractionating melt migrating along olivine grain boundaries. In such processes, Mg# and Ni content are "buffered" by exchange reactions with Mg, Fe, and Ni-rich olivine, whereas the abundance of incompatible elements such as Na—which preferentially partition into melt versus crystals—increases with decreasing melt mass (e.g., Kelemen, 1986).

In Figure **F4,** note that gabbroic rocks from very slow spreading ridges with thin crust (e.g., Cayman Rise) have the lowest anorthite content in plagioclase at a given olivine Mg#, whereas gabbroic rocks from the fast-spreading East Pacific Rise, sampled at Hess Deep, have the highest anorthite content for a given olivine Mg#. This variation has commonly been interpreted to indicate crystallization from primitive magmas with a variety of Na/Ca ratios, in turn reflecting a variety of different degrees of melting at different mantle potential temperatures, with high-Na magmas arising from low degrees of melting and low-Na magmas from high degrees of melting (e.g., Meyer et al., 1989). However, an alternative interpretation is that primitive Cayman magmas with high Na content arose as a result of extensive "reactive fractionation" in a thick thermal boundary layer, whereas Hess Deep magmas with much lower Na contents underwent little or no "reactive fractionation" in the shallow mantle, perhaps because the thermal boundary layer beneath the fast-spreading East Pacific Rise is very thin compared to that beneath the slow-spreading Cayman Rise.

Variation in the intensity of "reactive fractionation" has the potential to account for much of the variation in the sodium content of primitive mid-ocean-ridge basalts, which has hitherto been attributed to variations in mantle potential temperature. This hypothesis forms the basis for ongoing research (Collier and Kelemen, 2005, 2006). However, this work is not yet published, and we forego a more extensive summary here.

The pressure and temperature of equilibration between melt and a mineral assemblage including olivine, two pyroxenes, and plagioclase can be estimated from the melt composition using the method of Kinzler and Grove (1992). Rare earth element (REE) contents in Site 1275 poikilitic impregnated peridotites (Kelemen et al., submitted [**N1**]) are consistent with crystallization from "normal" MORB. Kelemen, Kikawa, Miller et al. (2004) and Kelemen et al. (submitted [**N1**]) used the composition of 87 primitive MORB glasses at 14°–16°N with Mg# 0.60–0.73 (from the Petrological Database of the Ocean Floor, PetDB, online at **petdb.ldeo.columbia.edu/petdb**). These primitive MORB glasses could be olivine + two pyroxene + plagioclase saturated at 0.54 GPa (±0.14 GPa, 2σ) and 1220°C (±16°C, 2σ) (Shipboard Scientific Party, 2004a: fig. F53 and accompanying text). Other proposed melt composition barometers yield similar results (Kelemen et al., submitted [**N1**]).

A variety of metamorphic reactions could occur during cooling and decompression of olivine–two pyroxene–plagioclase–spinel mineral assemblages. To the extent that minerals approach equilibrium during this process, thermodynamic data for minerals in these reactions can be used to estimate the pressure and temperature conditions for "closure," after which metamorphic reactions effectively ceased. The boundary between plagioclase and spinel lherzolite facies (e.g., Green and Hibberson, 1970) is defined by the reaction

$$MgAl_2O_4 + Mg_2Si_2O_6 + CaMgSi_2O_6 = 2Mg_2Si_2O_4 + CaAl_2Si_2O_8 \quad (1)$$

$MgAl_2O_4$ in spinel ss + enstatite in orthopyroxene + diopside in clinopyroxene =
2 forsterite in olivine + anorthite in plagioclase

that relates the activities of the most abundant mineral end-members in the olivine, orthopyroxene, clinopyroxene, and plagioclase solid solutions in our samples. Reaction 1, together with temperature estimates from independent geothermometers, has been used to estimate pressure in terrestrial and lunar olivine + 2 pyroxene + plagioclase + spinel assemblages (e.g., Frost, 1976; McCallum and Schwartz, 2001; Newman et al., 1999; Tartarotti et al., 2002).

To estimate closure conditions for Reaction 1 in impregnated peridotites from Site 1275, Kelemen et al. (submitted [N1]) used mineral solution models and internally consistent thermodynamic data for most mineral end-members from Holland and Powell (1998) and the Sack and Ghiorso (1991) solution model for Cr-Al-Fe-Mg spinels. An independent estimate of temperature was derived from the Lindsley and Anderson (1983) two-pyroxene solvus thermometer, as implemented in the computer program QUILF (Andersen et al., 1993). Two-pyroxene solvus temperatures based on clinopyroxene compositions, together with analytical uncertainty, range from ~1075° to 1110°C (with one sample representing an outlier at ~1215°C) ± 50°C. Other pyroxene solvus thermometers yielded consistent results, essentially independent of pressure. Combining these temperature estimates with Reaction 1, incorporating analytical uncertainty, yields pressures of 0.65 to 0.72 ± 0.1 GPa (1σ).

In summary, Kelemen et al. (submitted [N1]) concluded that metamorphic net transfer equilibria involving $MgAl_2O_4$, $Mg_2Si_2O_6$, $CaMgSi_2O_6$, $2Mg_2Si_2O_4$, and $CaAl_2Si_2O_8$ in impregnated peridotites from Site 1275 last equilibrated at pressures of ~0.68 ± 0.2 GPa and temperatures of 1100° ± 75°C. This estimate is consistent, within uncertainty, with isobaric cooling from the estimated igneous crystallization conditions for primitive MORB from this region, described above and in Kelemen, Kikawa, Miller, et al. (2004). Impregnated peridotites and olivine gabbronorites at Sites 1268, 1270, and 1271 contained olivine, two pyroxenes, and plagioclase, ± spinel, prior to alteration. They have similar whole-rock compositions to the impregnated peridotites at Site 1275 and so probably record similar conditions of crystallization.

Results of thermobarometry support the inference that igneous rocks crystallized and began to conductively cool at depths 15–20 km below the seafloor in the 14°–16°N region along the Mid-Atlantic Ridge. This result is consistent with previous estimates of the thermal boundary layer thickness beneath slow-spreading ridges based on thermal models (Braun et al., 2000; Reid and Jackson, 1981; Shen and Forsyth, 1995; Sleep, 1975). It is also consistent with geological inferences based on dredging and diving in the 14°–16°N region (e.g., Cannat, 1996; Cannat and Casey, 1995; Cannat et al., 1997) and with interpretation of the liquid lines of descent formed by spatially and genetically related mid-ocean-ridge basalts, which indicate cotectic crystallization at pressures of 0.4–0.6 GPa along parts of the Mid-Atlantic Ridge (Elthon, 1993; Grove et al., 1992; Meurer et al., 2001; Michael and Chase, 1987), including the 14°–16°N region (Xia et al., submitted [N2]). More generally, this result may also be consistent with suggestions that crystallization of cooling melt migrating by porous flow can modify the composition of many upper mantle peridotites beneath slow-spreading ridges (e.g., Dick, 1989; Niu, 1997).

Gabbroic Rock Compositions

As noted above, Kelemen et al. (submitted [N1]) also emphasize the evolved nature of most of the gabbroic rocks recovered during Leg 209. As shown in Figure F5 (modified from Shipboard Scientific Party 2004a: fig. F58), primitive MORB has an Mg# ~ 0.7 and ~50 ppm Zr, whereas average MORB has an Mg# ~ 0.6 and ~100 ppm Zr. If Zr were a perfectly incompatible element (concentration in crystal/liquid = 0), then doubling of Zr concentration would require 50% crystallization. In fact, Zr is not perfectly incompatible (concentration in crystal/liquid > 0), which suggests that average MORB is the product of >50% crystal fractionation. There should be a complementary reservoir of refractory high-Mg#, low-Zr cumulates formed by this crystal fractionation. Such a refractory cumulate reservoir is observed in the southern massifs of the Oman ophiolite (e.g., Pallister and Hopson, 1981). However, refractory cumulates are rare among gabbroic suites sampled from mid-ocean ridges. The average compositions of gabbroic rocks from ODP Hole 735B on the Southwest Indian Ridge (Natland and Dick, 2002) and ODP Leg 153 sites on the Mid-Atlantic Ridge (Agar and Lloyd, 1997) are similar to those of primitive MORB and thus cannot represent the refractory cumulate reservoir. Similarly, gabbroic plutons sampled during Leg 209 at Sites 1270, 1272, and 1275 are far too rich in iron to explain the variation trend of MORB.

F5. Molar Mg# vs. Zr in MORB and oceanic gabbros, p. 29.

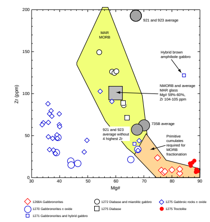

Only primitive gabbronorites at Site 1268 and impregnated peridotites at Sites 1268, 1270, 1271, and 1275 have appropriately high Mg# and low Zr to represent the refractory cumulate reservoir required by MORB variation. As noted above, these rocks, with their high Mg# and abundant orthopyroxene, probably formed at depths of 15 km or more. We infer that the more evolved gabbroic rocks sampled during Leg 209 formed at lower temperatures and shallower depths and thus that crystal fractionation is polybaric in the 14°–16°N region. Many of the more evolved gabbroic rocks are similar to MORB glass compositions and may not be cumulates at all. Additionally, some gabbroic rocks from Leg 209 are so evolved that they have no volcanic equivalents among MORB. We infer that a substantial proportion of the melts entering the thermal boundary layer in the 14°–16°N region crystallize entirely at depth, without any eruptive products on the seafloor.

Impregnation of Residual Peridotites

Seyler et al. (2007) discuss the origin of interstitial clinopyroxene in residual peridotites from Leg 209, commonly with symplectitic textures involving chromian spinel (e.g., see figures and associated text in Shipboard Scientific Party, 2004a: fig. F43; 2004b: figs. F10, F11; 2004c: fig. F24; 2004f: figs. F17–F22). Clinopyroxenes are also intergrown with magmatic sulfides whose composition and texture are presented for the first time in Seyler et al. (2007). These unusual clinopyroxenes are associated with anomalously high CaO contents at a given Al_2O_3 concentration (e.g., Shipboard Scientific Party, 2004f: fig. F51 and associated text).

Similarly, orthopyroxenes in residual peridotites from Leg 209 exhibit interstitial textures, apparent association with embayed olivine crystals, and coarse sympletitic intergrowths with spinel (see figures and associated text in Shipboard Scientific Party 2004b: figs. F6, F7, F9, F12, F44–F46, F77, F91; 2004c: figs. F19, F28, F38, F91; 2004d: fig. F42; 2004f: figs. F10–F16).

Using new major and trace element analyses of silicates and new analyses of sulfides, Seyler et al. (2007) conclude that the association of clinopyroxene, spinel, and sulfide minerals was produced by reaction between residual orthopyroxene and a melt saturated with respect to clinopyroxene and sulfur. The introduction of this melt into previously depleted residual peridotites produced these intergrowths and changed the bulk composition of the rocks. It is increasingly evident that many, if not most, residual peridotites recovered during dredging of the mid-ocean ridges have undergone some extent of "refertilization" by a process similar to that proposed by Seyler et al. (2007). For example, in a recent landmark paper, Niu (2004) showed that most dredged peridotites contain enrichments of highly incompatible elements that are not reflected in residual mineral compositions and yet involve fluid-immobile elements such as Nb, Ta, and Th, so probably result from addition of a late igneous phase along residual crystal grain boundaries, without equilibration with grain interiors.

Takazawa et al. (this volume) contributed a study of ultramafic and mafic rocks from Hole 1271B. Shipboard observations document the lithologic assemblage of predominantly dunite, with lesser brown amphibole gabbro, olivine gabbro, and troctolite, and a minor amount of harzburgite and olivine gabbronorite. The interpretation of the probable genesis of this assemblage was initial crystallization of plagioclase and clinopyroxene from basaltic liquid migrating along grain boundaries. As the section cooled the flow regime changed from porous media to fracture-focused flow, resulting in crystallization of mafic rocks in an ultramafic host. The results reported in Takazawa et al. (this volume) are consistent with this interpretation. They note a variance in Fo content of olivine between dunite (~89–91) and mafic rocks (~86–89) and a concomitant variability in chrome spinel compositions. This is attributed to more refractory olivine and spinel in the dunite owing to melt-rock reaction as the dunite represents a fossilized melt channel.

Metamorphism and Hydrothermal Alteration

Bach et al. (2004) reported on petrographic observations of alteration in peridotites from Leg 209, supplemented by thermodynamic modeling of fluid/rock reactions. Petrographic data in the paper summarize and add to extensive shipboard observations, made largely by the same group of authors (see the "Metamorphic Petrology" sections in each site chapter in Kelemen, Kikawa, Miller, et al., 2004). Serpentine and talc ± amphibole are observed and predicted in relatively SiO_2 rich residual harzburgites, whereas serpentine and brucite are observed and predicted in SiO_2-poor dunites. Alteration reactions controlled in large part by these bulk compositions probably controlled fluid pH, fO_2, and concentrations of dissolved species.

A notable exception to the rock-dominated alteration assemblages observed at most sites is the extensive replacement of early formed serpentine by talc at Site 1268. Some residual peridotite whole-rock compositions determined onboard the *JOIDES Resolution* were identical to stoichiometric talc, despite the fact that textures clearly indicated that the protoliths were olivine-rich, porphyroclastic, and protogranular harzburgites. Although it has long been known that some altered peridotites have low Mg/Si compared to unaltered protoliths, it is debated whether this is due to Mg removal (e.g., Snow and Dick, 1995) or SiO_2 addition (e.g., Boschi et al., 2006).

In the Site 1268 summary (Shipboard Scientific Party, 2004a: figs. F12, F13, and associated text), we argued that wholesale replacement of peridotite by talc at essentially constant Mg/Fe almost certainly involved addition of SiO_2 (adding ~40 wt% SiO_2 relative to the original rock mass). If, instead, the change was produced mainly by removal of Mg and Fe (removing at least 16 wt% of the original rock mass), it would be a dramatic coincidence for this process to preserve the original Mg/Fe ratio of the protolith. Bach et al. (2004) support our conclusion in the site summary, noting that the solubility of Mg in hydrothermal fluid is very low in the presence of hydrous Mg-Fe silicates at pH > 6, which is in the pH range that they calculate likely for fluids during serpentinization and subsequent talc alteration at Site 1268. However, they hedge their bet and invoke the need for further study. Doubtless, studies of sulfide mineralogy and, particularly, stable isotope thermometry on samples from this site are likely to shed further light on the conditions before and during talc alteration.

Pursuing the notion that SiO_2 was indeed added to harzburgites to produce the talc-rich rocks, Bach et al. (2004) suggest that the source of SiO_2 could have been the abundant gabbronorite intrusions into peridotite that were sampled at Site 1268. Some Site 1268 gabbronorites have indeed undergone metasomatism, most notably loss of CaO (Shipboard Scientific Party, 2004a: fig. F14C and associated text). However, in the Site 1268 summary we showed that SiO_2 contents in altered gabbronorites from Site 1268 are essentially identical to SiO_2 in fresh gabbronorite (Shipboard Scientific Party, 2004a: fig. F14), suggesting that the extent of SiO_2 leaching from gabbroic intrusions was minor compared to the extent of SiO_2 addition to peridotites. Furthermore, in some gabbronorite samples from Site 1268, orthopyroxene is pseudomorphically replaced by talc (Shipboard Scientific Party, 2004b: fig. F30 and associated text), which requires addition of SiO_2 to the pyroxene pseudomorphs. Thus, it seems unlikely that the gabbronorites that were actually sampled at Site 1268 were the source of the SiO_2 added to the talc-rich peridotites. Since gabbroic intrusions comprise <50% of the volume of core from Hole 1268A, we can infer that SiO_2 loss from the gabbronorites did not balance SiO_2 gain in the peridotites. In this view, the source of SiO_2 metasomatically added to the Site 1268 talc-altered peridotites has yet to be identified.

Paulick et al. (2006) interpret whole-rock major and trace element characteristics of peridotites recovered during Leg 209 in terms of residues of partial melting, igneous "impregnation," and metasomatism during hydrothermal alteration. Following Niu (2004), they ascribe variable light REE concentrations in samples from Site 1270 and 1271, not correlated with heavy REE concentrations, to igneous impregnation because the light REEs are correlated with concentrations of fluid-immobile high field strength elements and Th. This is in agreement with shipboard interpretation of thin section relationships and major element chemistry in terms of addition of igneous, "cumulate," interstitial plagioclase, and clinopyroxene, with or without hornblende, zircon, and other minor phases to depleted harzburgite and to plagioclase- and pyroxene-free dunite during porous flow of cooling, crystallizing melt in the shallow mantle beneath the Mid-Atlantic Ridge.

In contrast, Paulick et al. (2006) interpret light REE variation that is weakly correlated with both heavy REE *and* high field strength element concentrations in residual peridotite samples from Sites 1268, 1272, and 1274 to metasomatism during hydrothermal alteration. Within the peridotites from Sites 1268, 1272, and 1274, Paulick et al. (2006) find that "rock-dominated" serpentinization controlled the composition of most Site 1274 samples, with addition of H_2O and oxidation but little additional metasomatism during shallow melt migration or alteration. This may be somewhat at odds with the evidence for impregnation of igneous clinopyroxene in Site 1274 peridotites described by Seyler et al. (2007), whose results are summarized above.

Alteration strongly affected the composition of residual peridotites from Site 1268. Paulick et al. (2006) extensively describe the effects of "fluid-dominated" serpentinization at Site 1268, including "gains in sulfur and development of [a] U-shaped REE pattern with strong positive Eu anomalies." High-temperature fluids (350°–400°C) with these trace element characteristics are observed in hydrothermal vents (Paulick et al., 2006).

A third type of metasomatism during hydrothermal alteration, as delineated by Paulick et al. (2006), is associated with the replacement of olivine, pyroxene, and serpentine by talc at Site 1268, yielding smooth light REE–enriched trace element patterns with negative Eu anomalies.

Bach et al. (2006) reiterate observations on serpentinization parageneses and textures from the Leg 209 *Initial Reports* volume (Kelemen, Kikawa, Miller, et al., 2004), emphasizing that zones with comparatively high water-rock ratios (mesh rims and veins) contain serpentine plus magnetite, whereas zones with lower water-rock ratios (mesh cores and rims of relict olivine) contain serpentine plus brucite. High water-rock ratios result in both hydration and oxidation of the peridotite protolith, whereas olivine-rich protoliths with low water-rock ratios show only hydration. Both of these processes are potentially isochemical with regard to all species other than H_2O and oxygen. Bach et al. (2006) link these observations with shipboard measurements of magnetic properties and density; oxidized samples with abundant magnetite are denser and have more pronounced magnetic susceptibility than unoxidized samples containing brucite and no magnetite.

Moll et al. (this volume) report microprobe analyses of a variety of primary and alteration phases in peridotite samples from Leg 209. Primary minerals at Site 1274 are very "depleted" with high Fo contents in olivine and high Cr/Al in spinel, as anticipated from whole-rock compositions determined during Leg 209. As was clear during the cruise (e.g., Shipboard Scientific Party, 2004f: fig. F51 and accompanying text) and reiterated by Seyler et al. (2007)—described above—and Harvey et al. (2006)—summarized below—these are among the most depleted residual peridotites known along the mid-ocean ridges. In samples where pseudomorphs of olivine and orthopyroxene may be clearly distinguished, **Moll et al.** (this volume) analyzed alteration phases replacing these minerals. Although there are some differences between serpentines replacing olivine compared to those replacing pyroxene, the similarities are striking and suggest that major element cations were extensively redistributed during alteration. It is clear that the authors plan to publish a more complete analysis of the chemical changes associated with alteration at a later date, and one can anticipate that this will be very interesting.

Sulfide mineral compositions from Hole 1268A are reported by **Miller** (this volume). Sulfide mineral species change downsection from millerite and chalcopyrite in shallow cores to pyrrhotite and pentlandite with depth. The general downhole trend suggests sulfide mineral precipitation in conditions with decreasing sulfur and oxygen fugacity. This trend is interrupted coincident with cores that recovered a brecciated gabbroic intrusion. Sulfide minerals that indicate precipitation at relatively higher sulfur and oxygen fugacity as well as sphalerite occur in the central core of the intrusion breccia. Strongly contrasting pyrite compositions suggest at least two episodes of pyrite precipitation, but there is no clear morphological distinction between phases.

STRUCTURE AND TECTONICS

One of the main aims of Leg 209 was to measure ductile deformation fabrics in residual mantle peridotites in order to constrain the mode of mantle upwelling and corner flow beneath slow-spreading ridges. We hoped to use mineral shape fabrics, as well as lattice-preferred orientation of olivine, to determine whether ductile deformation was radial, consistent with three-dimensionally focused, buoyancy-driven upwelling, or orthogonal to the rift axis, consistent with two-dimensional, plate-driven upwelling. Our expectations were based on extensive observations of mineral shape fabrics in residual mantle peridotites; in particular, field and laboratory measurements of spinel and pyroxene lineation, together with laboratory observations of olivine elongation and subgrain orientation, have been used to map ductile deformation trajectories in the Oman ophiolite and other massifs (e.g., Nicolas et al., 1972; Nicolas and Violette, 1982).

Summary of Shipboard Observations

As noted above, the third important observation emphasized in our synthesis paper (Kelemen et al., submitted [N1]) was that most peridotites lacked textural evidence for subsolidus plastic deformation. Instead, shipboard observations indicated that in most peridotite both spinel and pyroxene form equant grains or irregular grains interstitial to olivine crystals (Shipboard Scientific Party, 2004b: figs. F6, F7, F9, F44; 2004c: figs. F19, F91; 2004d: fig. F38; 2004e: figs. F16, F42; 2004g: figs. F10-F15, and especially figs. F22 and F36). Spinel, in particular, forms skeletal grains whose extensions are commonly <100 µm wide but extend along olivine grain boundaries over millimeters in two and three dimensions. In some cases, these spinels are intergrown with pyroxene and could have been armored by "strong" pyroxene porphyroclasts during ductile deformation of olivine. However, in other samples the spinel was present along pyroxene-free olivine grain boundaries. Similarly, at every site we recovered peridotites in which pyroxenes are poikilitic or interstitial to olivine.

The shipboard structural geology team used a semiquantitative scale of crystal-plastic deformation intensity in peridotites, ranging from a lack of any crystal-plastic shape fabric (0, also called "protogranular"), through several stages of foliation and porphyroclast development, to mylonitic (4) and ultramylonitic (5) fabrics. Recovered peridotites from Site 1268 had an average deformation intensity of ~0.9, those from 1270 had an average intensity of ~1.2, from 1271, ~0.5, from 1272, ~0.2, and from 1274, ~0.3. Impregnated peridotites at Site 1275 had an average ductile deformation intensity <0.1. Omitting mylonitic rocks (crystal fabric intensity > 3), these averages become ~0.5 for Site 1268 and ~1 for Site 1270. Averages are not changed significantly by omitting mylonitic intervals for all other sites. In contrast, peridotites from ODP Site 895 at Hess Deep, deformed beneath the East Pacific Rise (e.g., Mével, Gillis, Allan, and Meyer, 1996), and from the intermediate- to fast-spreading Oman ophiolite (e.g., Nicolas et al., 2000; Nicolas and Violette, 1982) generally have well-developed spinel shape fabrics and discernable orthopyroxene shape fabrics, corresponding to a crystal-plastic deformation intensity of 2–3 on the shipboard scale used during Leg 209.

The presence of interstitial spinel without pyroxene, and interstitial pyroxene without spinel, virtually rules out subsolidus exsolution of spinel from pyroxene as the cause for the interstitial textures. Instead, we infer that the interstitial textures formed during melting, melt migration, igneous dissolution, and/or precipitation from melt migrating by porous flow along crystal grain boundaries. Given that these rocks, and mixtures of these peridotites with small amounts of primitive basaltic melt, have solidus temperatures >1200°C at 0.4–0.7 GPa (e.g., Hirschmann, 2000), we infer that most peridotites recovered by drilling during Leg 209 have not recorded measurable shear strain at temperatures <1200°C. Given the estimates for the thickness of the thermal boundary layer summarized in **"Thermobarometry,"** p. 4, above, this inference indicates that most peridotites recovered during Leg 209 were not penetratively deformed at depths less than ~20 km below the seafloor.

High-temperature (>900°C) mylonitic shear zones with recrystallized olivine, pyroxene, and/or plagioclase grain sizes 20–100 µm cut weakly deformed peridotites and gabbroic rocks at Sites 1268, 1270, 1271, and 1274. Illustrations can be found in the Leg 209 *Initial Reports* volume (Shipboard Scientific Party, 2004a: figs. F20, F22; 2004b: figs. F48, F49, F50; 2004c: figs. F12, F20, F21, F39, F51, F60, F65, F77, F80; 2004d: figs. F39, F41, F42 2004f: figs. F6, F40). These mylonites formed by localized high-strain ductile deformation. Many of the Leg 209 peridotite mylonitic shear zones are substantially coarser than peridotite mylonites previously dredged from the Mid-Atlantic Ridge that formed at ~600°C and high stress (e.g., Jaroslow et al., 1996). We infer that the coarser mylonites recovered during Leg 209 formed under lower stress conditions at temperatures >900°C because they have olivine grain sizes in the same range as in well-documented high-temperature shear zones in ophiolites and mantle massifs (Dijkstra et al., 2002; Kelemen and Dick, 1995; Newman et al., 1999; Vissers et al., 1991). Most, though not all, of the Leg 209 mylonites formed along contacts between residual peridotite and gabbroic rocks.

In addition to ductile shear zones, we recovered fault gouge and cataclasites at Sites 1268, 1270, 1271, 1272, 1274, and 1275. These formed in numerous brittle fault zones (Shipboard Scientific Party, 2004a: figs. F41, F48; 2004b: figs. F57, F58, F64; 2004d: fig. F53; 2004e: figs. F47, F48; 2004f: figs. F7, F32, F47, F48; 2004g: figs. F56–F60).

It is striking that we recovered samples from more than one ductile shear zone at Sites 1268, 1270, and 1271 and more than one brittle fault zone at Sites 1268, 1270, 1271, 1272, and 1274. In addition, based on bathymetry and dive observations, at Sites 1270, 1274,and 1275 the seafloor is interpreted as a fault surface. Thus, several zones of localized deformation were recovered at all gabbro and peridotite sites except Site 1275, where only one significant fault—at the seafloor—was observed. This indicates that the "typical" spacing between adjacent shear zones and faults in the 14°–16°N region—at least close to the seafloor—is <100–200 m.

Shipboard and Shore-Based Analysis of Paleomagnetic Data

Garcés and Gee (2007) synthesized paleomagnetic data from Leg 209 core using shipboard observations (Kelemen, Kikawa, Miller, et al., 2004) and subsequent shore-based laboratory analyses. Expanding on a hypothesis formed at sea (Shipboard Scientific Party, 2004a: figs. F16, F17, F18, F28, F29, F30, and accompanying text), Garcés and Gee (2007) demonstrate that large tectonic rotations (>90°) have occurred in the footwall(s) to currently low-angle faults recovered in core and thus that the paleomagnetic data are consistent with nucleation and slip along high-angle normal faults, followed by passive rotation of the high-angle faults to their current, nearly horizontal orientations. Original fault orientations dipped steeply toward the spreading axis.

Lattice-Preferred Orientation of Minerals in Site 1274 Peridotite

In their 2005 American Geophysical Union abstract, Achenbach et al. report on preliminary measurements of olivine and pyroxene lattice-preferred orientation in a few samples from Hole 1274A. They find a weak shape foliation in olivine and orthopyroxene and weakly developed olivine lattice fabrics consistent with dislocation creep at ~1200°C with flow in or near the plane of the foliation. Using paleomagnetic data and assumptions about ridge-parallel tectonic rotation (e.g., Garcés and Gee, 2007; Kelemen, Kikawa, Miller, et al., 2004) they attempt to restore the microstructural observations to their geographical orientation at the time that the remnant magnetization was acquired (probably, during serpentinization at ~200°–300°C). They conclude that there was subhorizontal foliation with horizontal ridge-parallel olivine a-axis lineation at the time of magnetization. With the additional assumption that there were no significant tectonic rotations of the rocks during the time for cooling from ~1200°C to ~300°C, these results are consistent with high-temperature ridge-parallel ductile flow in the mantle beneath the Mid-Atlantic Ridge near Site 1274.

Discussion of Structure and Tectonics Results

The geometry of plate spreading, together with the observation of residual mantle peridotites and high-pressure igneous cumulates on the seafloor, demands that some rocks underwent tectonic uplift and rotation during corner flow within the upper 15–20 km below the seafloor. The paucity of ductile deformation fabrics in most peridotites, coupled with the abundance of localized mylonitic shear zones and faults, suggests that blocks of peridotite were passively uplifted and rotated along localized shear zones extending deeper than 15 km. Whereas some faults observed in the region, particularly at Site 1275, could have formed at shallow depth—for example, at the "dike–gabbro transition" as inferred by Escartín et al. (2003) for this same area—denudation of nearly undeformed residual peridotites and high-pressure cumulates requires uplift along localized shear zones and faults that extend to depths of more than 15 km.

The 14°–16°N region along the Mid-Atlantic Ridge has commonly been interpreted as unusual. Numerous studies have documented the presence of extensive outcrops of mantle peridotite on both sides of the rift valley, extending for at least 50 km from the 15°20′ Fracture Zone (summarized in Kelemen, Kikawa, Miller, et al., 2004), whereas along other geologically well known parts of the Mid-Atlantic Ridge, exposed mantle peridotite is typically limited to one side of the rift valley, generally on inside corner highs within 10–30 km of a large-offset fracture zone (e.g., Tucholke and Lin, 1994). Thus, although peridotite exposures along the Mid-Atlantic Ridge are commonly interpreted as the result of asymmetric deformation along detachment faults, it has generally been thought that the 14°–16°N region is tectonically more complex (with alternating dips of normal faults) and "magma starved."

For this reason, the processes outlined in the previous section of this paper—igneous crystallization and localized deformation throughout a thermal boundary layer >15 km thick beneath the Mid-Atlantic Ridge—could be unique to this unusual area. However, as noted above, theoretical calculations suggest that the thermal boundary layer beneath most or all slow-spreading ridges could extend deeper than 15 km, and petrological studies of lavas suggest that mantle-derived melts begin to crystallize at depths of 15 km or more in many places along the Mid-Atlantic Ridge. In addition, shipboard observations during Leg 209 suggest that localized shear zones form along contacts between residual peridotite and gabbroic intrusions, perhaps because the rheological contrast between peridotite and gabbro enhances localization of deformation between ~1200° and 600°C. Thus, Kelemen et al. (submitted [**N1**]) suggest that the 14°–16°N area may simply be an end-member example that reveals typical slow-spreading processes in their best known, clearest expression.

In this context, Kelemen et al. (submitted [**N1**]) question some of the common interpretations of this region. For example, is this area really "magma starved"? Leg 209 observations, coupled with previous work, suggest that the entire 14°–16°N area may be underlain by mantle peridotite hosting 20%–40% gabbroic intrusions and impregnations. Gabbro of 30% in the upper 21 km of an oceanic plate would correspond to 7 km of "normal" oceanic crust. Gabbro of 30% (7.2 km/s) + 75% peridotite (8.2 km/s) yields a "mantle" compressional wave velocity (V_P) (7.9 km/s) greater than or equal to sub-Mohorovicic Discontinuity (Moho) V_P observed in about half of the seismic refraction studies of oceanic crust that have been conducted to date (Shipboard Scientific Party, 2004a: fig. F8 and associated references).

Recently, Lizarralde et al. (2004) performed a refraction experiment along a flow line in the Atlantic south of Bermuda. They found that an episode of relatively slow spreading formed seismic crust ~5 km thick, compared to 7-km-thick crust formed at faster spreading rates. Shallow mantle V_P is slower beneath the 5-km-thick crust, compared to that beneath the 7-km-thick crust. The difference in V_P is consistent with the presence of ~7.5% gabbroic material distributed within the uppermost mantle beneath the 5-km-thick crust, so that the total proportion of gabbroic rocks formed during the slower and faster spreading episodes could be the same. Furthermore, Lizarralde et al. (2004) observed that areas with 5-km-thick crust had Bouger gravity anomalies 20–30 mGal higher than areas with 7-km-thick crust, even though the proportion of gabbroic rocks could be the same in both areas. They modeled the gravity data for the area with 5-km-thick crust as the result of 7.5% gabbroic material distributed over 30–60 km of the uppermost mantle. Generalizing from this result, Kelemen et al. (submitted [**N1**]) hypothesized that some of the observed variation of seismic crustal thickness and Bouger gravity anomalies along the Mid-Atlantic Ridge may be due to variable depth and distribution of gabbroic intrusions rather than to variable overall proportions of gabbroic rocks.

Finally, the strength of seismic anisotropy in the shallow mantle—formed by alignment of olivine a-axes during viscous deformation—will be smaller where corner flow in the uppermost mantle is accommodated by block rotation along localized shear zones, rather than by penetrative ductile deformation of high-temperature peridotites. At fast-spreading ridges, where the adiabatic geotherm probably extends to the base of the crust, corner flow in the shallow mantle is probably accommodated entirely by ductile deformation of all peridotites (e.g., Nicolas et al., 2000). Beneath slow-spreading ridges, localized deformation and passive rotation of undeformed blocks is likely in the uppermost mantle (Fig. F6). Thus, during Leg 209, we hypothesized that seismic anisotropy in the upper 15–30 km of the mantle would be greater beneath crust formed at the fast-spreading East Pacific Rise compared to the slow-spreading Mid-Atlantic Ridge. We were delighted to discover that this hypothesis is consistent with the recent results of Gaherty et al. (2004).

F6. Igneous accretion and seafloor spreading at fast- vs. slow-spreading ridges, p. 30.

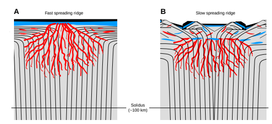

Amplifying the paleomagnetic results and shipboard observations of shear zone and fault structure, Schroeder et al. (submitted [N3]) present a tectonic synthesis of data from Leg 209. They endorse a "rolling hinge" model for large normal faults that denude mantle peridotite, intruded by gabbroic plutons, to the seafloor, coupled with later development of other normal faults with smaller displacement.

To summarize, recent seismic and gravity observations of old Atlantic seafloor southwest of Bermuda independently suggest that gabbroic material is distributed throughout the uppermost mantle below the Moho during periods of relatively slow spreading and that the role of penetrative ductile deformation is much smaller in the shallow mantle beneath the Atlantic compared to the Pacific. These interpretations are consistent with the central results from Leg 209. Thus, many or most slow-spreading ridges may be characterized by igneous crystallization and localized deformation throughout a thermal boundary layer thicker than 15 km. Continued geological and geophysical studies can test this hypothesis and help to define the regional extent of oceanic plates that form in this way.

CONTRIBUTIONS TO GLOBAL GEOCHEMISTRY

Osmium Isotope Geochemistry

Harvey et al. (2006) present new Os isotopic data, together with other new geochemical data, on residual peridotites recovered from Site 1274. They also provide an excellent summary of Os isotope data from previous studies of oceanic peridotites, sulfides in peridotites, and MORB glasses. All of the 20 peridotite samples analyzed record $^{187}Os/^{188}Os$ less radiogenic than proposed for "primitive upper mantle" (PUM), indicating an ancient depletion event, probably more than 1 billion years ago. Although abyssal peridotites with $^{187}Os/^{188}Os$ lower than PUM have been observed previously, the mean of previous data is close to PUM, whereas the Site 1274 data are consistently lower than PUM. The unradiogenic Os isotope ratios in Site 1274 samples range as low as 0.117, slightly lower than the previous minimum value of 0.118 observed in mid-ocean-ridge peridotites (Standish et al., 2002).

Sulfide grains from the least radiogenic peridotite sample from Site 1274 generally have $^{187}Os/^{188}Os$ consistent with the whole-rock value. A few radiogenic grains have low Os and high Re. A few single sulfide grains show lower $^{187}Os/^{188}Os$ ratios than the most depleted whole-rock values, as low as 0.114, indicating that—whereas overall Os isotope ratios may have been raised by melt-rock or seawater-rock interaction—some samples record an ancient Re depletion event. This event can be modeled as having occurred more than 2 billion years ago. These data confirm the observation of $^{187}Os/^{188}Os$ as low as 0.110 in hydrothermal fluid from the Juan de Fuca Ridge (Sharma et al., 2000), indicating a highly depleted, ancient mantle component in the mantle source of mid-ocean-ridge basalts.

It remains unclear why there is so much variability in $^{187}Os/^{188}Os$ in the Site 1274 peridotites (0.11691–0.12665). The least radiogenic sample is only 12 m from the sample with the third highest $^{187}Os/^{188}Os$ and <30 m from the most radiogenic sample. Either (1) the mantle in the melting region beneath the Mid-Atlantic Ridge is variable in $^{187}Os/^{188}Os$ on a ~10-m scale and/or (2) tectonic processes have juxtaposed peridotites from larger heterogeneous domains in the melting region and/or (3) melt/rock reaction during MORB transport from source to surface has created small-scale $^{187}Os/^{188}Os$ variation in shallow mantle peridotites and/or (4) interaction with seawater has substantially modified whole-rock Os isotope values in Site 1274 peridotites. The fact that no observed MORB $^{187}Os/^{188}Os$ values extend significantly below those proposed for the primitive upper mantle suggests that source rocks rich in radiogenic Os play an important role in mantle melting, and thus that the variability in Os isotope ratios in Site 1274 peridotite is due mainly to igneous processes (1, 2, and 3) and not to hydrothermal alteration of homogeneous residues with low Os isotope ratios.

Trace Element Geochemistry and the Pb Paradox

As illustrated in Figure F7, Godard et al. (2005) find consistent high Pb/Ce in inductively coupled plasma–mass spectroscopic (ICP-MS) data for a compilation of the least altered and/or impregnated residual peridotite compositions from Leg 209 (Paulick et al., 2006). High Pb/Ce is also observed in abyssal peridotites from mid-ocean ridges worldwide (Niu, 2004), together with Godard and Kelemen's unpublished data on peridotites from the Oman, Josephine, and Trinity ophiolites and the Jurassic Talkeetna arc (Leg 209 and Oman ICP-MS data from the Université de Montpellier; Josephine, Trinity, and Talkeetna from Washington State University; some Pb concentrations checked by isotope dilution at Woods Hole Oceanographic Institution). Although this work is not yet published, we expand upon these observations and their interpretation here.

F7. MORB-normalized trace elements in residual harzburgites, p. 31.

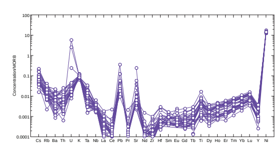

The samples in the Godard et al. (2005) compilation have average Pb/Ce ~10 times higher than primitive mantle (Hofmann, 1988), with only 3 of 180 samples having Pb/Ce less than that in primitive mantle. REE abundance, and Ce concentration specifically, is less than that in primitive mantle in 165 of 180 samples, consistent with depletion via melt extraction, modified by some magmatic refertilization. High Pb concentrations could be due to (1) retention of Pb in residual sulfide, (2) addition of Pb in sulfide and plagioclase during "impregnation" by crystallizing melt, and/or (3) addition of Pb in sulfide and carbonate during alteration.

There is little doubt that Pb is an incompatible element during melting of the mantle to form mid-ocean-ridge basalt with a bulk rock/melt distribution coefficient similar to that of Ce, and thus “unadulterated” residues should be depleted in Pb relative to primitive mantle and should have Pb/Ce approximately equal to Pb/Ce in mid-ocean-ridge basalts. Therefore, retention of Pb in residual sulfide during melt extraction cannot be the main cause of high Pb/Ce in residual peridotites. Additionally, Pb concentration is not well correlated with compatible and moderately incompatible elements such as Ni, Cr, Ti, and heavy REE.

Pb concentration is strongly positively correlated with Th, Nb, and light REE. These elements are commonly considered “immobile” during hydrothermal alteration (e.g., Winchester and Floyd, 1977) but mobile during melt migration and igneous metasomatism. Thus, high Pb concentrations and Pb/Ce are most likely due to magmatic impregnation—“reactive fractionation” in the shallow mantle—whereas metasomatism during hydrothermal alteration probably does not play an important role in Pb enrichment.

All of the residual peridotite samples in the Godard et al. (2005) compilation, except those from the Talkeetna arc section, have Th/Pb and Th/Nb less than those in primitive mantle. This suggests that relatively high Th concentration may distinguish arc from ridge (and ophiolite) peridotites. More importantly from the perspective of global geochemistry, this indicates that recycled mid-ocean-ridge peridotites will evolve to low $^{208}Pb/^{204}Pb$ compared to the primitive mantle over long residence times in the mantle.

Most dredged mid-ocean-ridge peridotites worldwide (Niu, 2004) have high U concentrations and U/Pb higher than in primitive mantle, but most other samples in our compilation have U/Pb less than in primitive mantle. Three shallow, oxidized residual peridotites recovered via drilling during Leg 209 have high U concentrations; U concentrations in other Leg 209 residual peridotites are lower than in MORB and primitive mantle (Fig. F8). Thus, high U in dredged mid-ocean-ridge peridotites can most likely be attributed to oxidizing seafloor weathering. Given that oxidized weathering only extends tens of meters below the seafloor, Godard et al. (2005) inferred that most mid-ocean-ridge peridotites have Th/Pb and U/Pb less than in primitive mantle. If residual peridotites form with Pb isotope ratios similar to mid-ocean-ridge basalts, these rocks will evolve to $^{206}Pb/^{204}Pb$ and $^{207}Pb/^{204}Pb$ ratios less radiogenic than primitive mantle.

F8. MORB-normalized U in residual harzburgites, p. 32.

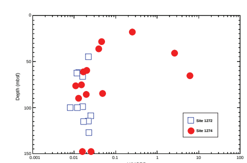

The effect of subduction modification on Th/Pb and U/Pb is unclear. If Pb is immobile during hydrothermal alteration—as suggested by the positive correlation of Pb concentration with Th, Nb, and light REE—then subduction modification of Pb concentrations is likely to be minor as well. If U is fluid-mobile in subduction zones and is removed by fluids evolved from subducting peridotite, this will lower U/Pb and modified residues will evolve to still lower $^{206}Pb/^{204}Pb$ and $^{207}Pb/^{204}Pb$ ratios.

As discussed elsewhere in this paper, crystallization of igneous phases from cooling melt migrating along peridotite grain boundaries may be common in the thick conductive boundary layer beneath slow-spreading ridges. These crystallizing phases likely include sulfide and plagioclase with abundant Pb. Beneath the Mid-Atlantic Ridge, such reactive fractionation of sulfide and plagioclase is likely to occur within a 20-km-thick conductive boundary layer. Based on this estimate, together with the observation that residual peridotite samples in the Godard et al. (2005) compilation contain Pb concentrations similar to those in primitive mantle, tens of percent of mantle Pb could be sequestered in a high-Pb residual peridotite reservoir over geologic time. Evolution of strongly unradiogenic Pb isotope ratios in such a reservoir, in refractory peridotites that contribute little to subsequent melting, offers a potential solution to the "first lead paradox," in which observed mid-ocean-ridge and ocean-island lavas are systematically enriched in radiogenic Pb compared to meteorites and the inferred bulk earth composition (Allègre, 1969).

Zircon Provenance (Ridge vs. Arc Zircons)

Grimes et al. (in press) report on a new method of trace element discrimination for distinguishing zircons formed at mid-ocean ridges versus those formed in arc environments. This method will be useful for determining the provenance of detrital zircons in the geologic record, including the Archean and Hadean detrital zircons that provide virtually the only samples of Earth's crust prior to 3.8 billion years ago. Grimes et al. (in press) found that, as for ridge versus arc lavas, zircons from ridge environments have low fractionation-corrected U and Th concentrations compared to zircons from arc environments. This result contrasts with that of several previous studies, most recently that of Coogan and Hinton (2006), which used REE and Ti concentration data to argue that zircons from different tectonic environments could not be distinguished using trace element data. Using the new discrimination diagrams, ancient zircons from the Jack Hills and Acasta localities show clear affinities with arc zircons and are distinct from zircon generated in a mid-ocean-ridge environment.

GEOBIOLOGY

Josef et al. (this volume) found no measurable microbial enhancement of olivine dissolution rate as measured using dissolved Li and Si for as long as 709 days. It had been hypothesized that microbes might mediate reaction of olivine with water, capitalizing on the chemical potential energy inherent in the disequilibrium between mantle olivine and surface waters. If so, microbial activity might enhance olivine dissolution rates. Moeseneder et al. (unpubl. data) inoculated sterile basalt glass and sterile olivine with bacteria cultured from pillow lavas and observed an enhancement in dissolution rates via high Li and Si in solution, compared to sterile controls. Josef et al. (this volume) did not culture microorganisms from Leg 209 peridotite samples, so the presence of microbial matter in these samples is not certain. Thus, the lack of enhancement of dissolved Li and Si in their samples, compared to sterilized controls, could be due to a variety of factors including a lack of living microbes in the samples.

AEROBIOLOGY

Griffin et al. (2006) describe observations of "dust-borne" microorganisms collected from the derrick of the *JOIDES Resolution* during Leg 209. Colony-forming units of bacteria and fungi were detected. Satellite imagery indicated high dust concentrations emanating from North African sources during the time that the most dust and the largest number of colony-forming units were collected on the *JOIDES Resolution*.

ACKNOWLEDGMENTS

We are very grateful for the help of numerous ODP and TransOcean personnel during Leg 209 shipboard operations. We would particularly like to thank Mike Storms, Roy Davis, Paula Weiss, and Lisa Crowder from ODP and Wayne Malone, Pepe Estevez, Nick Parish, Phil Christie, and Dwight Mossman from TransOcean. Many scientists provided unpublished data without which Leg 209 would not have been possible. These include Henri Bougault, Peter Rona, Leonid Dmitriev, Sergei Silantiev, Mathilde Cannat, John Collins, Bob Detrick, members of the Woods Hole Oceanographic Institution/Japan Agency for Marine-Earth Science and Technology (WHOI/JAMSTEC) MODE 98 scientific party and their collaborators (especially Toshi Fujiwara, Mike Braun, and Jian Lin), and the scientific party of *James Clark Ross* Cruise JR63 (especially Chris MacLeod and Javier Escartín). Karen Hanghøj helped with ion microprobe analyses of rare earth elements in clinopyroxene. The WHOI Geochemistry Seminar, especially Greg Hirth, Stan Hart, and Nobu Shimizu, provided helpful criticism and advice. This research used samples and/or data provided by the Ocean Drilling Program (ODP). ODP is sponsored by the U.S. National Science Foundation and participating countries under management of Joint Oceanographic Institutions (JOI), Inc. In addition to research support from ODP, P.B. Kelemen was supported in this work in part by NSF research grants EAR-0538143, OCE-0426160, OCE-0405572, EAR-0409092, OCE-0327588, EAR-0337677, OCE-0242233, OCE-0137327, and OCE-0118572.

REFERENCES

Achenbach, K.L., Faul, U., Cheadle, M., and Swapp, S., 2005. Testing models of mantle upwelling: microstructure, crystallography, and seismic anisotropy of peridotites from 15 degrees N, Mid-Atlantic Ridge. *Eos, Trans. Am. Geophys. Union,* 86(52)(Suppl.):T41D-1327. (Abstract)

Agar, S.M., and Lloyd, G.E., 1997. Deformation of Fe-Ti oxides in gabbroic shear zones from the MARK area. *In* Karson, J.A., Cannat, M., Miller, D.J., and Elthon, D. (Eds.), *Proc. ODP, Sci. Results,* 153: College Station, TX (Ocean Drilling Program), 123–141. **doi:10.2973/odp.proc.sr.153.009.1997**

Allègre, C.J., 1969. Comportement des systèmes U-Th-Pb dans le manteau supérieur et modèle d'evolution de ce dernier au cours des temps géologiques. *Earth. Planet. Sci. Lett.,* 5:261–269. **doi:10.1016/S0012-821X(68)80050-0**

Andersen, D.J., Lindsley, D.H., and Davidson, P.M., 1993. QUILF: a Pascal program to assess equilibria among Fe-Mg-Mn-Ti oxides, pyroxenes, olivine, and quartz. *Comp. Geosci.,* 19(9):1333–1350. **doi:10.1016/0098-3004(93)90033-2**

Bach, W., Garrido, C.J., Paulick, H., Harvey, J., and Rosner, M., 2004. Seawater-peridotite interactions: first insights from ODP Leg 209, MAR 15°N. *Geochem., Geophys., Geosyst.,* 5(9):Q09F26. **doi:10.1029/2004GC000744**

Bach, W., Paulick, H., Garrido, C.J., Ildefonse, B., Meurer, W.P., and Humphris, S.E., 2006. Unraveling the sequence of serpentinization reactions: petrography, mineral chemistry, and petrophysics of serpentinites from MAR 15°N (ODP Leg 209, Site 1274). *Geophys. Res. Lett.,* 33(13):L13306. **doi:10.1029/2006GL025681**

Boschi, C., Früh-Green, G.L., Delacour, A., Karson, J.A., and Kelley, D.S., 2006. Mass transfer and fluid flow during detachment faulting and development of an oceanic core complex, Atlantis Massif (MAR 30°N). *Geochem., Geophys., Geosyst.,* 7(1):Q01004. **doi:10.1029/2005GC001074**

Braun, M.G., Hirth, G., and Parmentier, E.M., 2000. The effects of deep damp melting on mantle flow and melt generation beneath mid-ocean ridges. *Earth Planet. Sci. Lett.,* 176(3–4):339–356. **doi:10.1016/S0012-821X(00)00015-7**

Cannat, M., 1996. How thick is the magmatic crust at slow spreading oceanic ridges? *J. Geophys. Res.,* 101(B2):2847–2858. **doi:10.1029/95JB03116**

Cannat, M., Chatin, F., Whitechurch, H., and Ceuleneer, G., 1997. Gabbroic rocks trapped in the upper mantle at the Mid-Atlantic Ridge. *In* Karson, J.A., Cannat, M., Miller, D.J., and Elthon, D. (Eds.), *Proc. ODP, Sci. Results,* 153: College Station, TX (Ocean Drilling Program), 243–264. **doi:10.2973/odp.proc.sr.153.013.1997**

Cannat, M., and Casey, J.F., 1995. An ultramafic lift at the Mid-Atlantic Ridge: successive stages of magmatism in serpentinized peridotites from the 15N region. *In* Vissers, R.L.M., and Nicolas, A. (Eds.), *Mantle and Lower Crust Exposed in Oceanic Ridges and Ophiolites:* Dordrecht (Kluwer), 5–34.

Casey, J.F., 1997. Comparison of major- and trace-element geochemistry of abyssal peridotites and mafic plutonic rocks with basalts from the MARK region of the Mid-Atlantic Ridge. *In* Karson, J.A., Cannat, M., Miller, D.J., and Elthon, D. (Eds.), *Proc. ODP, Sci. Results,* 153: College Station, TX (Ocean Drilling Program), 181–241. **doi:10.2973/odp.proc.sr.153.012.1997**

Collier, M.L., and Kelemen, P.B., 2005. Are ultramafic 'assimilants' modifying MORB? *Eos, Trans. Am. Geophys. Union,* 86(52)(Suppl.):T41E-1355. (Abstract)

Collier, M.L., and Kelemen, P.B., 2006. Reactive crystal fractionation and MORB chemical variability: observations, theory, models, implications. *Eos, Trans. Am. Geophys. Union,* 87(52)(Suppl.):V23E-0693. (Abstract)

Coogan, L.A., and Hinton, R.W., 2006. Do the trace element compositions of detrital zircons require Hadean continental crust? *Geology,* 34(8):633–636. **doi:10.1130/G22737.1**

Dick, H.J.B., 1989. Abyssal peridotites, very slow spreading ridges and ocean ridge magmatism. *In* Saunders, A.D., and Norry, M.J. (Eds.), *Magmatism in the Ocean Basins*. Geol. Soc. Spec. Publ., 42:71–105.

Dick, H.J.B., Ozawa, K., Meyer, P.S., Niu, Y., Robinson, P.T., Constantin, M., Hebert, R., Natland, J.H., Hirth, G., and Mackie, S.M., 2002. Primary silicate mineral chemistry of a 1.5-km section of very slow spreading lower ocean crust: ODP Hole 735B, Southwest Indian Ridge. *In* Natland, J.H., Dick, H.J.B, Miller, D.J., and Von Herzen, R.P. (Eds.), *Proc. ODP, Sci. Results,* 176: College Station, TX (Ocean Drilling Program), 1–60. **doi:10.2973/odp.proc.sr.176.001.2002**

Dijkstra, A.H., Drury, M.R., and Frijhoff, R.M., 2002. Microstructures and lattice fabrics in the Hilti mantle section (Oman ophiolite): evidence for shear localization and melt weakening in the crust–mantle transition zone? *J. Geophys. Res.,* 107(B11):2270. **doi:10.1029/2001JB000458**

Elthon, D., 1987. Petrology of gabbroic rocks from the Mid-Cayman Rise spreading center. *J. Geophys. Res.,* 92:658–682.

Elthon, D., 1993. Crystallization of mid-ocean ridge basalts at moderate to high pressures. *Eur. J. Mineral.,* 5:1025–1037.

Escartín, J., Mével, C., MacLeod, C.J., and McCaig, A.M., 2003. Constraints on deformation conditions and the origin of oceanic detachments, the Mid-Atlantic Ridge core complex at 15°45′N. *Geochem., Geophys., Geosyst.,* 4(8):1067. **doi:10.1029/2002GC000472**

Frost, B.R., 1976. Limits to the assemblage forsterite-anorthite as inferred from peridotite hornfelses, Icicle Creek, Washington. *Am. Mineral.,* 61:732–750.

Gaherty, J.B., Lizarralde, D., Collins, J.A., Hirth, G., and Kim, S., 2004. Mantle deformation during slow seafloor spreading constrained by observations of seismic anisotropy in the western Atlantic. *Earth Planet. Sci. Lett.,* 228(3–4):255–265. **doi:10.1016/j.epsl.2004.10.026**

Garcés, M., and Gee, J.S., 2007. Paleomagnetic evidence of large footwall rotations associated with low-angle faults at the Mid-Atlantic Ridge. *Geology,* 35(3):279–282, **doi:10.1130/G23165A.1**

Garrido, C. J., Kelemen, P.B., and Hirth, G., 2001. Variation of cooling rate with depth in lower crust formed at an oceanic spreading ridge: plagioclase crystal size distributions in gabbros from the Oman ophiolite. *Geochem., Geophys., Geosyst.,* 2(10). **doi:10.1029/2000GC000136**

Godard, M., Kelemen, P., Hart, S., Jackson, M., and Hanghøj, K., 2005. High Pb/Ce reservoir in depleted, altered mantle peridotites. *Eos, Trans. Am. Geophys. Union,*86(52)(Suppl.):V32D-07. (Abstract)

Green, D.H., and Hibberson, W., 1970. The instability of plagioclase in peridotite at high pressure. *Lithos,* 3(3):209–221. **doi:10.1016/0024-4937(70)90074-5**

Griffin, D.W., Westphal, D.L., and Gray, M.A., 2006. Airborne microorganisms in the African desert dust corridor over the Mid-Atlantic Ridge, Ocean Drilling Program, Leg 209. *Aerobiologia,* 22(3):211–226. **doi:10.1007/s10453-006-9033-z**

Grimes, C.B., John, B.E., Kelemen, P.B., Mazdab, F.K., Wooden, J.L., Cheadle, M.J., Hanghoj, K., and Schwartz, J.J., in press. The trace element chemistry of zircons from oceanic crust: a method for distinguishing detrital zircon provenance. *Geology.*

Grove, T.L., Kinzler, R.J., and Bryan, W.B., 1992. Fractionation of mid-ocean ridge basalt (MORB). *In* Morgan, J.P., Blackman, D.K., and Sinton, J.M. (Eds.), *Mantle Flow and Melt Generation at Mid-Ocean Ridges*. Geophys. Monogr., 71:281–310.

Harvey, J., Gannoun, A., Burton, K.W., Rogers, N.W., Alard, O., and Parkinson, I.J., 2006. Ancient melt extraction from the oceanic upper mantle revealed by Re-Os isotopes in abyssal peridotites from the Mid-Atlantic Ridge. *Earth Planet. Sci. Lett.,* 244(3–4):606–621. **doi:10.1016/j.epsl.2006.02.031**

Hirschmann, M.M., 2000. Mantle solidus: experimental constraints and the effects of peridotite composition. *Geochem., Geophys., Geosyst.,* 1(10). **doi:10.1029/2000GC000070**

Hofmann, A.W., 1988. Chemical differentiation of the Earth: the relationship between mantle, continental crust, and oceanic crust. *Earth Planet. Sci. Lett.,* 90(3):297–314. **doi:10.1016/0012-821X(88)90132-X**

Holland, T.J.B., and Powell, R., 1998. An internally consistent thermodynamic data set for phases of petrological interest. *J. Metamorph. Geol.,* 16:309–343.

Jaroslow, G.E., Hirth, G., and Dick, H.J.B., 1996. Abyssal peridotite mylonites: implications for grain-size sensitive flow and strain localization in the oceanic lithosphere. *Tectonophysics,* 256(1–4):17–37. **doi:10.1016/0040-1951(95)00163-8**

Kelemen, P.B., 1986. Assimilation of ultramafic rocks in subduction-related magmatic arcs. *J. Geol.,* 94:829–843.

Kelemen, P.B., Braun, M.G., and Hirth, G., 2000. Spatial distribution of melt conduits in the mantle beneath oceanic spreading ridges: observations from the Ingalls and Oman ophiolites. *Geochem., Geophys., Geosyst.,* 1(7). **doi:10.1029/1999GC000012**

Kelemen, P.B., and Dick, H.J.B., 1995. Focused melt flow and localized deformation in the upper mantle: juxtaposition of replacive dunite and ductile shear zones in the Josephine peridotite, SW Oregon. *J. Geophys. Res.,* 100(B1):423–438. **doi:10.1029/94JB02063**

Kelemen, P.B., Kikawa, E., Miller, D.J., et al., 2004. *Proc. ODP, Init. Repts.,* 209: College Station, TX (Ocean Drilling Program). **doi:10.2973/odp.proc.ir.209.2004**

Kelemen, P.B., Koga, K., and Shimizu, N., 1997. Geochemistry of gabbro sills in the crust–mantle transition zone of the Oman ophiolite: implications for the origin of the oceanic lower crust. *Earth Planet. Sci. Lett.,* 146(3–4):475–488. **doi:10.1016/S0012-821X(96)00235-X**

Kinzler, R.J., and Grove, T.L., 1992. Primary magmas of mid-ocean ridge basalts, 2. Applications. *J. Geophys. Res.,* 97:6907–6926.

Koga, K.T., Kelemen, P.B., and Shimizu, N., 2001. Petrogenesis of the crust–mantle transition zone and the origin of lower crustal wehrlite in the Oman ophiolite. *Geochem., Geophys., Geosyst.,* 2(9). **doi:10.1029/2000GC000132**

Korenaga, J., and Kelemen, P.B., 1997. Origin of gabbro sills in the Moho transition zone of the Oman ophiolite: implications for magma transport in the oceanic lower crust. *J. Geophys. Res.,* 102(B12):27729–27749. **doi:10.1029/97JB02604**

Korenaga, J., and Kelemen, P.B., 1998. Melt migration through the oceanic lower crust: a constraint from melt percolation modeling with finite solid diffusion. *Earth Planet. Sci. Lett.,* 156(1–2):1–11. **doi:10.1016/S0012-821X(98)00004-1**

Lindsley, D.H., and Andersen, D.J., 1983. A two-pyroxene thermometer. *J. Geophys. Res.,* 88(B1):A887–A906.

Lizarralde, D., Gaherty, J.B., Collins, J.A., Hirth, G., and Kim, S.D., 2004. Spreading-rate dependence of melt extraction at mid-ocean ridges from mantle seismic refraction data. *Nature (London, U. K.),* 432(7018):744–747. **doi:10.1038/nature03140**

McCallum, I.S., and Schwartz, J.M., 2001. Lunar Mg suite: thermobarometry and petrogenesis of parental magmas. *J. Geophys. Res.,* 106(E11):27969–27984. **doi:10.1029/2000JE001397**

Meurer, W.P., Sturm, M.A., Klein, E.M., and Karson, J.A., 2001. Basalt compositions from the Mid-Atlantic Ridge at the SMARK area (22°30′N to 22°50′N)—implications for parental liquid variability at isotopically homogeneous spreading centers. *Earth Planet. Sci. Lett.,* 186(3–4):451–469. **doi:10.1016/S0012-821X(01)00260-6**

Mével, C., Gillis, K.M., Allan, J.F., and Meyer, P.S., 1996. *Proc. ODP, Sci. Results,* 147: College Station, TX (Ocean Drilling Program). **doi:10.2973/odp.proc.sr.147.1996**

Meyer, P.S., Dick, H.J.B., and Thompson, G., 1989. Cumulate gabbros from the Southwest Indian Ridge, 54°S–7°16′E: implications for magmatic processes at a slow spreading ridge. *Contrib. Mineral. Petrol.,* 103(1):44–63. **doi:10.1007/BF00371364**

Michael, P.J., and Chase, R.L., 1987. The influence of primary magma composition, H_2O and pressure on mid-ocean ridge basalt differentiation. *Contrib. Mineral. Petrol.,* 96(2):245–263. **doi:10.1007/BF00375237**

Natland, J.H., and Dick, H.J.B., 1996. Melt migration through high-level gabbroic cumulates of the East Pacific Rise at Hess Deep: the origin of magma lenses and the deep crustal structure of fast-spreading ridges. *In* Mével, C., Gillis, K.M., Allan, J.F., and Meyer, P.S. (Eds.), *Proc. ODP, Sci. Results,* 147: College Station, TX (Ocean Drilling Program), 21–58. **doi:10.2973/odp.proc.sr.147.002.1996**

Natland, J.H., and Dick, H.J.B., 2002. Stratigraphy and composition of gabbros drilled in Ocean Drilling Program Hole 735B, Southwest Indian Ridge: a synthesis of geochemical data. *In* Natland, J.H., Dick, H.J.B., Miller, D.J., and Von Herzen, R.P. (Eds.), *Proc. ODP, Sci. Results,* 176: College Station, TX (Ocean Drilling Program), 1–69. **doi:10.2973/odp.proc.sr.176.002.2002**

Newman, J., Lamb, W.M., Drury, M.R., and Vissers, R.L.M., 1999. Deformation processes in a peridotite shear zone: reaction-softening by an H_2O-deficient, continuous net transfer reaction. *Tectonophysics,* 303(1–4):193–222. **doi:10.1016/S0040-1951(98)00259-5**

Nicolas, A., Bouchez, J.L., and Boudier, F., 1972. Interpretation cinematique des deformations plastiques dans le massif de lherzolite de lanzo (Alpes piemontaises)—comparaison avec d'autres massifs. *Tectonophysics,* 14(2):143–171. **doi:10.1016/0040-1951(72)90107-2**

Nicolas, A., Boudier, F., Ildefonse, B., and Ball, E., 2000. Accretion of Oman and United Arab Emirates ophiolite—discussion of a new structural map. *Mar. Geophys. Res.,* 21(3–4):147–180. **doi:10.1023/A:1026769727917**

Nicolas, A., and Violette, J.F., 1982. Mantle flow at oceanic spreading centers: models derived from ophiolites. *Tectonophysics,* 81(3–4)319–339. **doi:10.1016/0040-1951(82)90136-6**

Niu, Y., 1997. Mantle melting and melt extraction processes beneath ocean ridges: evidence from abyssal peridotites. *J. Petrol.,* 38(8):1047–1074. **doi:10.1093/petrology/38.8.1047**

Niu, Y., 2004. Bulk-rock major and trace element compositions of abyssal peridotites: implications for mantle melting, melt extraction and post-melting processes beneath mid-ocean ridges. *J. Petrol.,* 45(12):2423–2458. **doi:10.1093/petrology/egh068**

Pallister, J.S., and Hopson, C.A., 1981. Samail ophiolite plutonic suite: field relations, phase variation, cryptic variation and layering, and a model of a spreading ridge magma chamber. *J. Geophys. Res.,* 86:2593–2644.

Paulick, H., Bach, W., Godard, M., De Hoog, J.C.M., Suhr, G., and Harvey, J., 2006. Geochemistry of abyssal peridotites (Mid-Atlantic Ridge, 15°20′N, ODP Leg 209): implications for fluid/rock interaction in slow spreading environments. *Chem. Geol.,* 234(3–4):179–210. **doi:10.1016/j.chemgeo.2006.04.011**

Reid, I., and Jackson, H.R., 1981. Oceanic spreading rate and crustal thickness. *Mar. Geophys. Res.,* 5:165–172.

Sack, R.O., and Ghiorso, M.S., 1991. Chromian spinels as petrogenetic indicators: thermodynamics and petrological applications. *Am. Mineral.,* 76:827–847.

Seyler, M., Lorand, J.-P., Dick, H.J.B., and Drouin, M., 2007. Pervasive melt percolation reactions in ultra-depleted refractory harzburgites at the Mid-Atlantic Ridge, 15°20′N: ODP Hole 1274A. *Contrib. Mineral. Petrol,* 153(3):303–319. **doi:10.1007/s00410-006-0148-6**

Sharma, M., Wasserburg, G.J., Hofmann, A.W., and Butterfield, D.A., 2000. Osmium isotopes in hydrothermal fluids from the Juan de Fuca Ridge. *Earth Planet. Sci. Lett.,* 179(1):139–152. **doi:10.1016/S0012-821X(00)00099-6**

Shen, Y., and Forsyth, D.W., 1995. Geochemical constraints on initial and final depths of melting beneath mid-ocean ridges. *J. Geophys. Res.,* 100(B2):2211–2238. **doi:10.1029/94JB02768**

Shipboard Scientific Party, 2004a. Leg 209 summary. *In* Kelemen, P.B., Kikawa, E., Miller, D.J., et al., *Proc. ODP, Init. Repts.,* 209: College Station TX (Ocean Drilling Program), 1–139. **doi:10.2973/odp.proc.ir.209.101.2004**

Shipboard Scientific Party, 2004b. Site 1268. *In* Kelemen, P.B., Kikawa, E., Miller, D.J., et al., *Proc. ODP, Init. Repts.,* 209: College Station, TX (Ocean Drilling Program), 1–171. **doi:10.2973/odp.proc.ir.209.103.2004**

Shipboard Scientific Party, 2004c. Site 1270. *In* Kelemen, P.B., Kikawa, E., Miller, D.J., et al., *Proc. ODP, Init. Repts.,* 209: College Station, TX (Ocean Drilling Program), 1–188. **doi:10.2973/odp.proc.ir.209.105.2004**

Shipboard Scientific Party, 2004d. Site 1271. *In* Kelemen, P.B., Kikawa, E., Miller, D.J., et al., *Proc. ODP, Init. Repts.,* 209: College Station, TX (Ocean Drilling Program), 1–129. **doi:10.2973/odp.proc.ir.209.106.2004**

Shipboard Scientific Party, 2004e. Site 1272. *In* Kelemen, P.B., Kikawa, E., Miller, D.J., et al., *Proc. ODP, Init. Repts.,* 209: College Station, TX (Ocean Drilling Program), 1–134. **doi:10.2973/odp.proc.ir.209.107.2004**

Shipboard Scientific Party, 2004f. Site 1274. *In* Kelemen, P.B., Kikawa, E., Miller, D.J., et al., *Proc. ODP, Init. Repts.,* 209: College Station, TX (Ocean Drilling Program), 1–116. **doi:10.2973/odp.proc.ir.209.109.2004**

Shipboard Scientific Party, 2004. Site 1275g. *In* Kelemen, P.B., Kikawa, E., Miller, D.J., et al., *Proc. ODP, Init. Repts.,* 209: College Station, TX (Ocean Drilling Program), 1–167. **doi:10.2973/odp.proc.ir.209.110.2004**

Sleep, N.H., 1975. Formation of oceanic crust: some thermal constraints. *J. Geophys. Res.,* 80:4037–4042.

Snow, J.E., and Dick, H.J.B., 1995. Pervasive magnesium loss by marine weathering of peridotite. *Geochim. Cosmochim. Acta,* 59(20):4219–4235. **doi:10.1016/0016-7037(95)00239-V**

Standish, J.J., Hart, S.R., Blusztajn, J., Dick, H.J.B., and Lee, K.L., 2002. Abyssal peridotite osmium isotopic compositions from Cr-spinel. *Geochem., Geophys., Geosyst.,* 3(1):1004. **doi:10.1029/2001GC000161**

Tartarotti, P., Susini, S., Nimis, P., and Ottolini, L., 2002. Melt migration in the upper mantle along the Romanche Fracture Zone (equatorial Atlantic). *Lithos,* 63(3–4):125–149. **doi:10.1016/S0024-4937(02)00116-0**

Tucholke, B.E., and Lin, J., 1994. A geological model for structure of ridge segments in slow spreading ocean crust. *J. Geophys. Res.,* 99(B6):11937–11958. **doi:10.1029/94JB00338**

Vissers, R.L.M., Drury, M.R., Hoogerduijn Strating, E.H., and van der Wal, D., 1991. Shear zones in the upper mantle: a case study in an Alpine lherzolite massif. *Geology,* 19(10):990–993. **doi:10.1130/0091-7613(1991)019<0990:SZITUM>2.3.CO;2**

Winchester, J.A., and Floyd, P.A., 1977. Geochemical discrimination of different magma series and their differentiation products using immobile elements. *Chem. Geol.,* 20:325–343. **doi:10.1016/0009-2541(77)90057-2**

Figure F1. Drill site locations for Leg 209. Inset of Mid-Atlantic Ridge bathymetry (base image from www.ngdc.noaa.gov/mgg/image/2minrelief.html) noting location of 15°20′N Fracture Zone modified from Kelemen, Kikawa, Miller, et al. (2004).

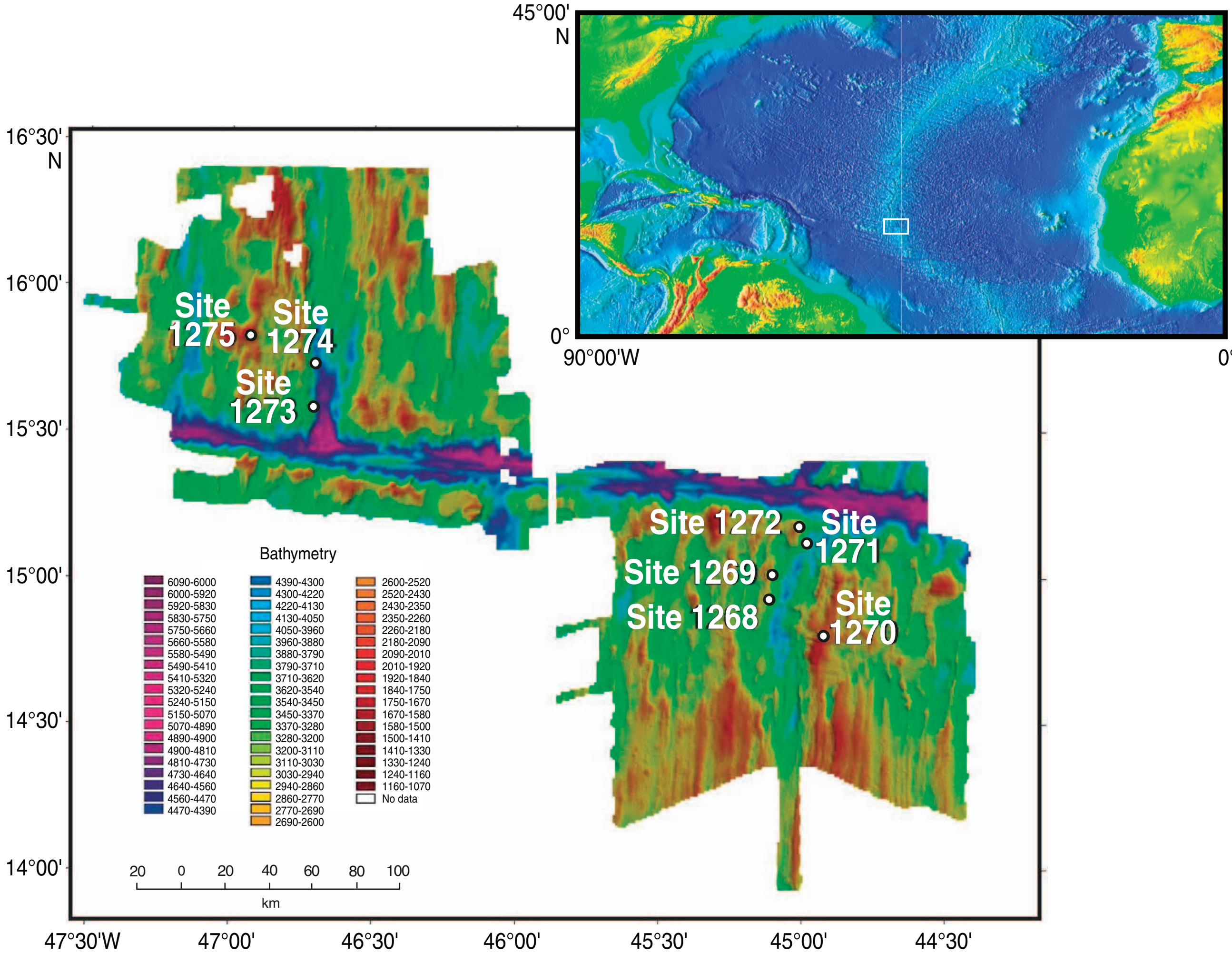

Figure F2. Simplified core logs for Sites 1268, 1270, 1271, 1272, 1274, and 1275 (detailed lithologic sections are available in Shipboard Scientific Party, 2004a: figs. F7, F21, F31, F37, F42, F50). Based on these data, we infer that the entire area may be underlain by mantle peridotite with ~20%–40% gabbroic intrusions and impregnations, consistent with results of previous dredging and submersible studies.

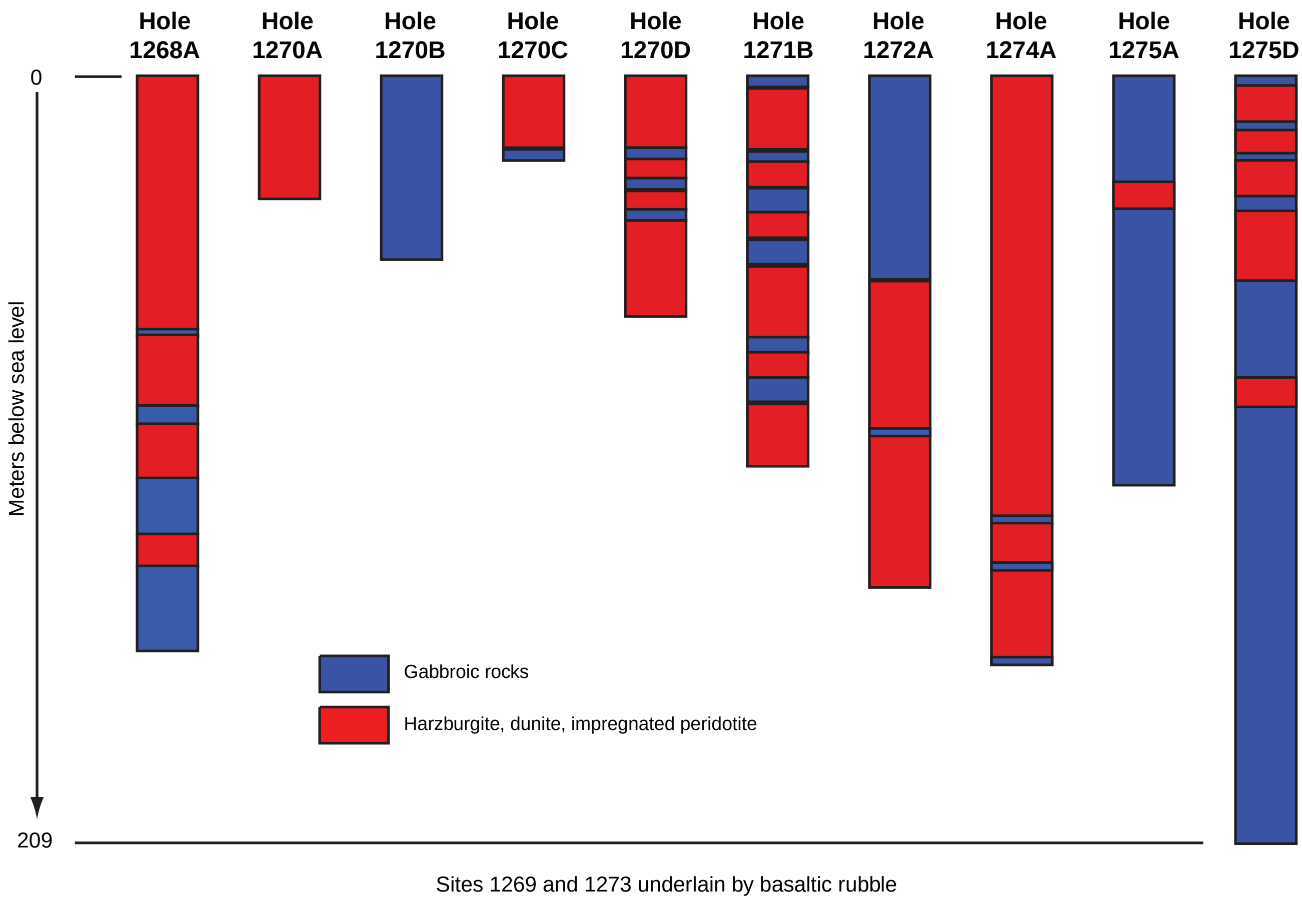

Figure F3. Poiklitic impregnated peridotite with olivine, plagioclase (plag), orthopyroxene (opx), clinopyroxene (cpx), and spinel (sp) showing "equilibrated" textures overprinted by low-temperature alteration along grain boundaries (Sample 209-1275B-7R-1, 75–80 cm) (cross-polarized light; field of view ~ 2.5 mm).

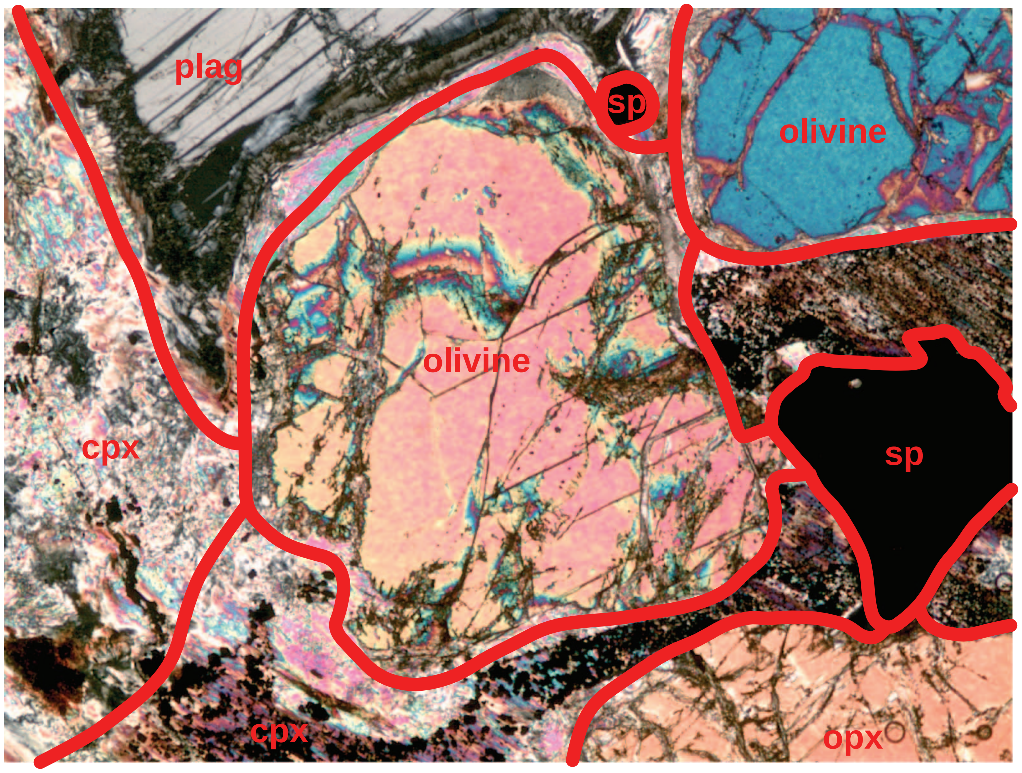

Figure F4. Normative anorthite in plagioclase (approximately molar Ca/[Ca+Na]) vs. forsterite in olivine (molar Mg/[Mg+Fe], or Mg#) in poikilitic impregnated peridotites from Site 1275, compared to compositions of plagioclase and olivine in gabbro sample suites from mid-ocean ridges and the Samail and Wadi Tayin massifs of the Oman ophiolite. The broad variation of anorthite content in plagioclase at nearly constant olivine forsterite content is probably due to "reactive fractionation" (i.e., reaction between residual peridotite and crystallizing melt migrating along olivine grain boundaries) (e.g., Kelemen, 1986). Comparative data on mid-ocean-ridge gabbro suites show the correlation of anorthite in plagioclase with forsterite in olivine that is expected for crystal fractionation without reaction with residual peridotite. Sources for comparative data on oceanic gabbro suites: Cayman Rise (Elthon, 1987); Hess Deep, East Pacific Rise (Natland and Dick, 1996); Mid-Atlantic Ridge Kane Fracture Zone (MARK) area Hole 923A (Casey, 1997); Southwest Indian Ridge Hole 735B (SWIR; Dick et al., 2002); and Samail and Wadi Tayin massifs of the Oman ophiolite (Garrido et al., 2001; Kelemen et al., 1997; Koga et al., 2001; Korenaga and Kelemen, 1997, 1998; Pallister and Hopson, 1981).

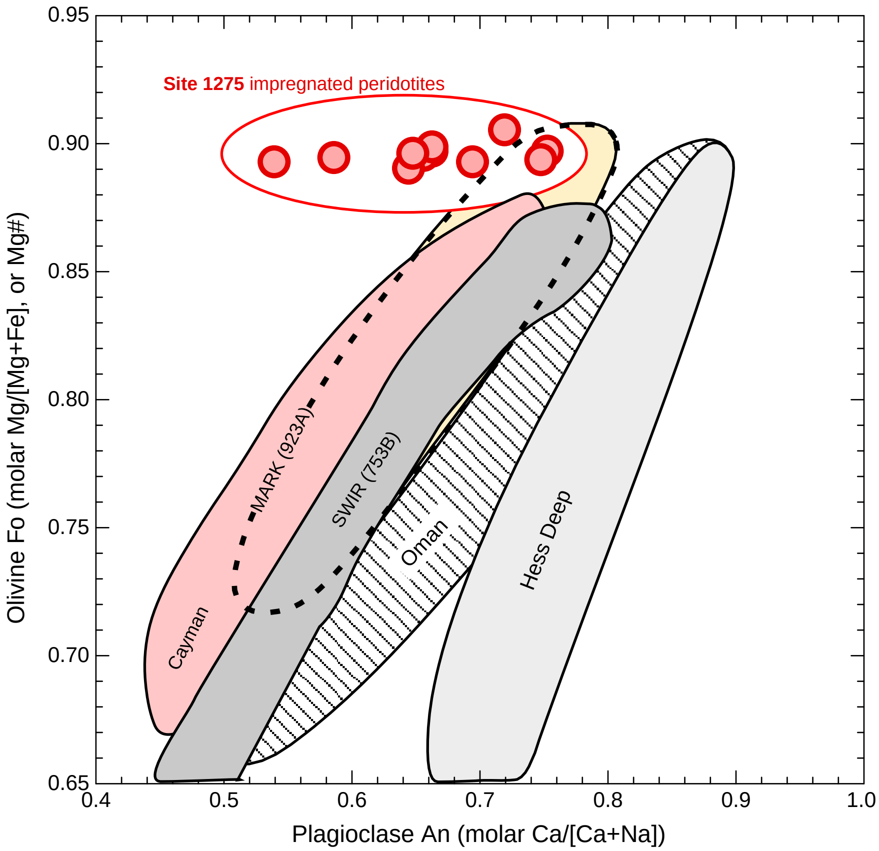

Figure F5. Molar Mg# (Mg/[Mg+Fe]) vs. Zr concentration in mid-ocean-ridge basalt (MORB) and oceanic gabbro samples. MORB glass data were downloaded in April 2003 from PetDB (**petdb.ldeo.Columbia.edu/petdb**). Other data: "average" normal MORB (NMORB; Hofmann, 1988); average composition of gabbroic rocks from ODP Hole 735B on the Southwest Indian Ridge (Natland and Dick, 2002); and average composition of gabbroic rocks from ODP Leg 153 on the Mid-Atlantic Ridge (MAR; Agar and Lloyd, 1997).

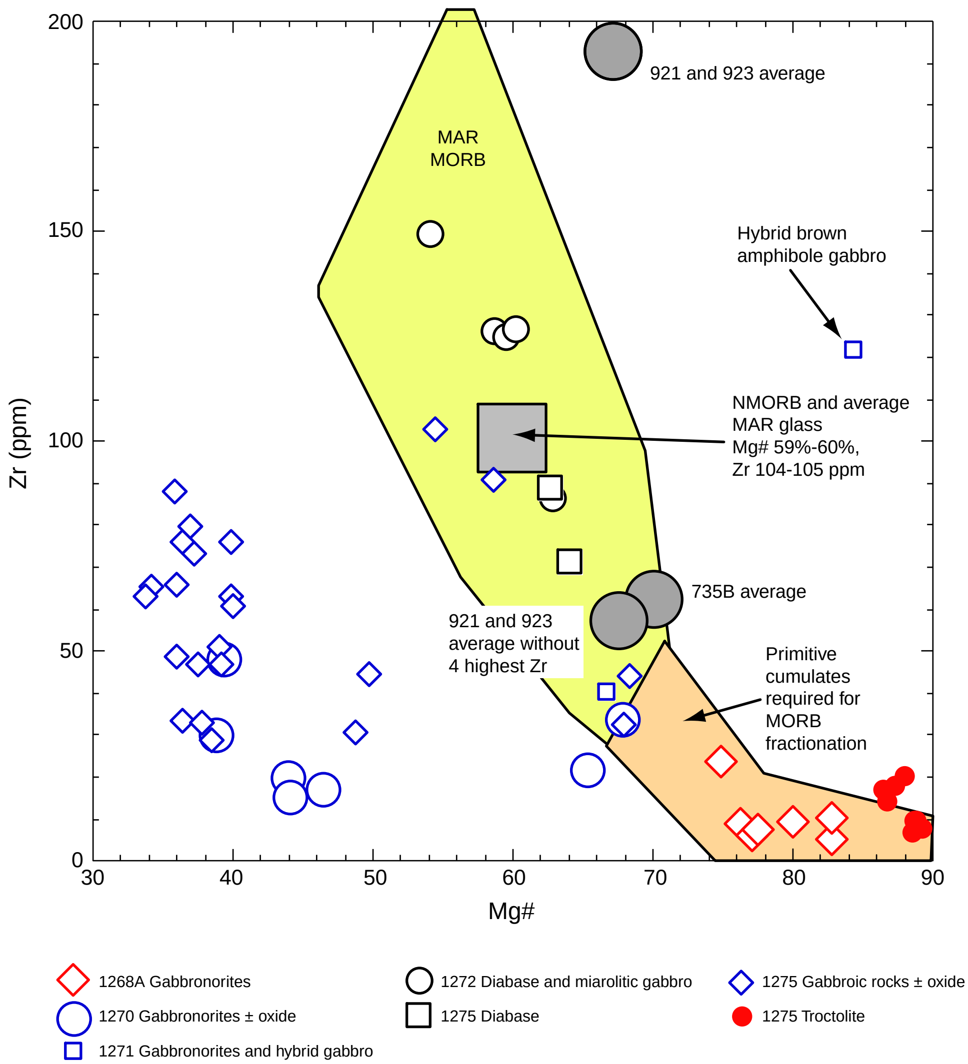

Figure F6. Synoptic diagram illustrating the inferred difference between igneous accretion and seafloor spreading at fast- vs. slow-spreading ridges. Lightest pattern represents residual peridotites. Red areas represent dunites formed as conduits for melt transport in the shallow mantle. Blue areas represent gabbroic plutonic rocks. Black areas represent volcanic rocks. **A.** Based in part on observations in the Oman ophiolite, where impregnated peridotites and gabbroic plutons are rare in the mantle section more than ~500 m below the crust–mantle transition zone and where plate spreading in the shallow mantle is accommodated by penetrative ductile deformation of residual peridotites (Kelemen et al., 2000). We infer that this represents a medium- to fast-spreading ridge, where the conductive boundary layer beneath the ridge axis does not extend far below the base of igneous crust. **B.** A hypothetical end-member scenario for igneous accretion and seafloor spreading at a slow-spreading ridge, based on our synthesis of results from Leg 209, together with other previous and ongoing research as described in the text. Impregnated peridotites and gabbroic plutons begin to form at the base of the conductive boundary layer, >15 km below the seafloor. Throughout much of this conductive boundary layer, at less than ~1100° or 1000°C, plate spreading is accommodated by localized deformation along mylonitic shear zones and—at lower temperatures—brittle faults. These shear zones and faults rotate and uplift passive blocks of residual peridotite that host gabbroic intrusions, some of which are exposed on the seafloor. In such a scenario, the thickness of igneous crust above the seismic Moho will be less than at fast-spreading ridges, and—because of the lack of penetrative deformation and the variable magnitude tectonic rotation—seismic anisotropy in the uppermost mantle will be less than in plates formed at fast-spreading ridges.

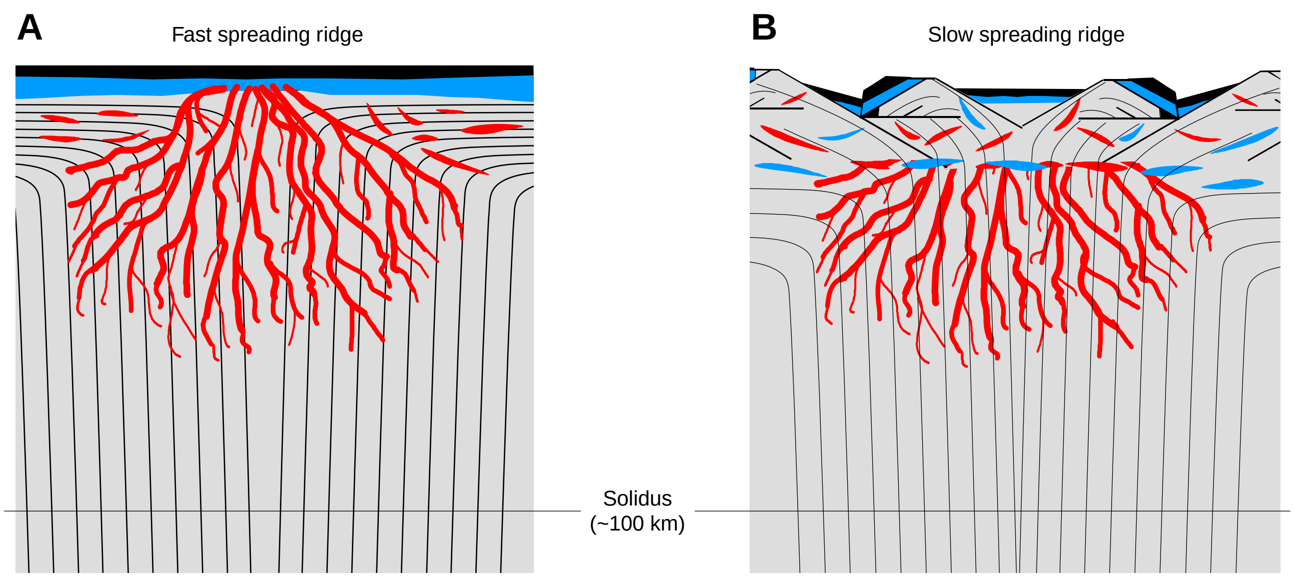

Figure F7. Trace element concentrations determined by Marguerite Godard using ICP-MS at the Université de Montpellier (as reported in Paulick et al., 2006) for residual harzburgites from Sites 1272 and 1274, excluding dunites and petrographically evident impregnated peridotites, normalized to mid-ocean-ridge basalt (MORB) concentrations (Hofmann, 1988).

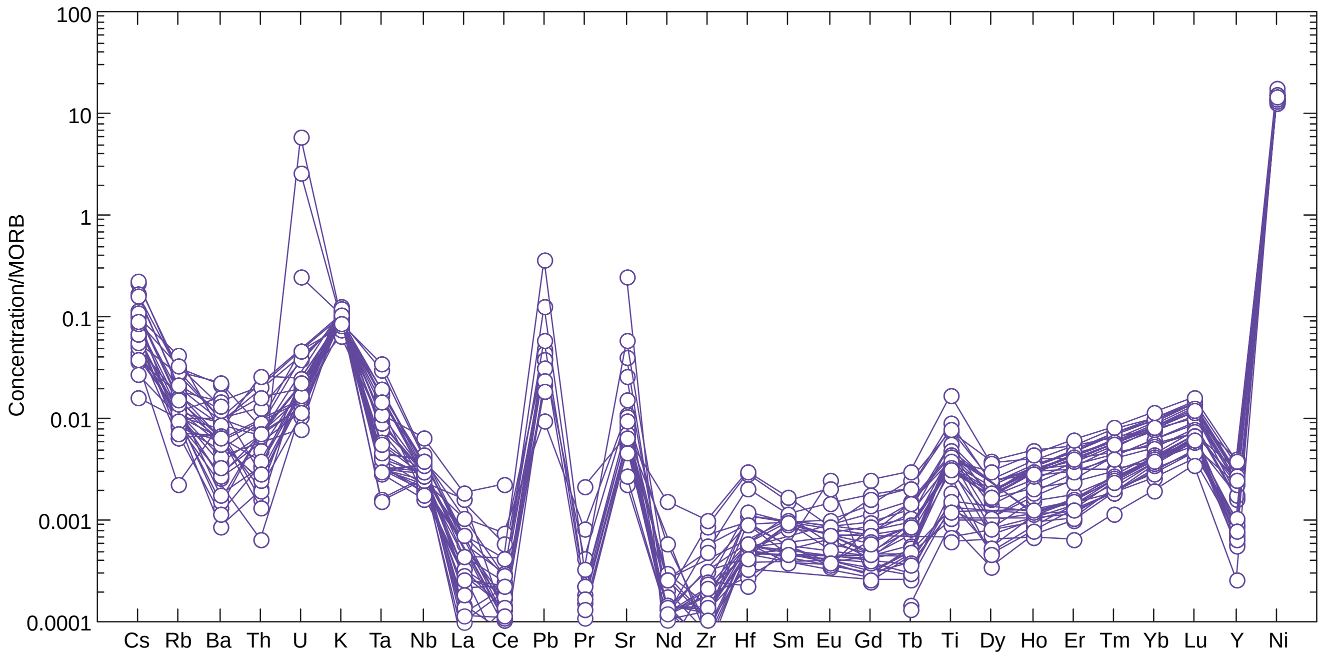

Figure F8. Mid-ocean-ridge basalt (MORB)-normalized U concentration for residual harzburgites from Sites 1272 and 1274. MORB normalization factors from Hofmann (1988).

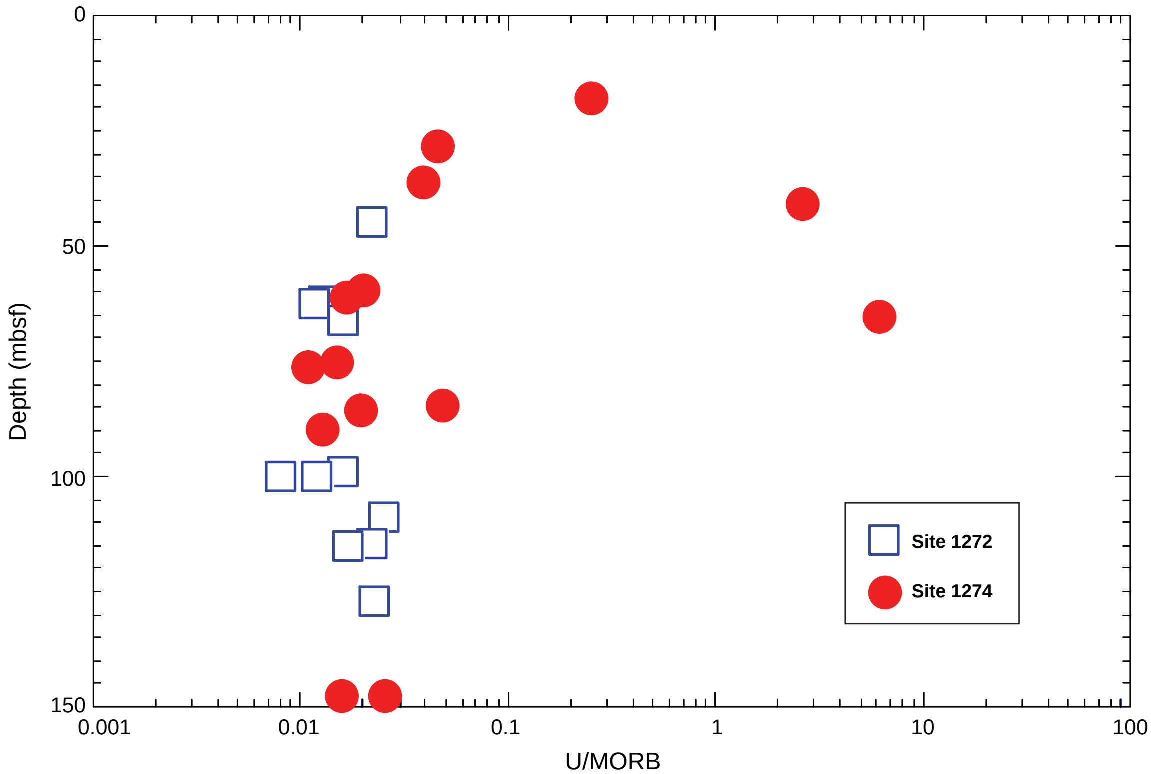

CHAPTER NOTES*

N1. Kelemen, P.B., Kikawa, E., Miller, D.J., and Party, S.S., submitted. Igneous crystallization and localized deformation in a thick thermal boundary layer beneath the slow-spreading Mid-Atlantic Ridge: results from ODP Leg 209. *Nature (London, U. K.).*

N2. Xia, C., Casey, J., Silantyev, S., Dmitriev, L., and Bougault, H., submitted. Geochemistry and petrogenesis of mid-ocean ridge basalts from 12 to 16N, Mid-Atlantic Ridge. *J. Geophys. Res.*

N3. Schroeder, T., Cheadle, M.J., Dick, H.J.B., Faul, U., Casey, J.F., and Kelemen, P.B., submitted. Non-volcanic seafloor spreading and corner-flow rotation accommodated by extensional faulting at 15N on the Mid-Atlantic Ridge: a structural synthesis of ODP Leg 209. *Geochem., Geophys., Geosyst.*

*Dates reflect file corrections or revisions.